R-99-16

Gas generation in SFL 3-5 and effects on radionuclide release

Kristina Skagius, Maria Lindgren, Karin Pers
Kemakta Konsult AB

December 1999

Svensk Kärnbränslehantering AB
Swedish Nuclear Fuel
and Waste Management Co
Box 5864
SE-102 40 Stockholm Sweden
Tel 08-459 84 00
+46 8 459 84 00
Fax 08-661 57 19
+46 8 661 57 19

ISSN 1402-3091
SKB Rapport R-99-16

Gas generation in SFL 3-5 and effects on radionuclide release

Kristina Skagius, Maria Lindgren, Karin Pers
Kemakta Konsult AB

December 1999

Keywords: Deep repository, LILW, Gas generation, Pressure build-up, Water displacement, Radionuclide release

Abstract

A deep repository, SFL 3-5, is presently planned for disposing of long-lived low- and intermediate-level waste. In this study the amounts of gas that can be generated in the waste packages and in the vaults are estimated. The potential gas pressure build-up, the displacement of contaminated water and the consequences on radionuclide release from the engineered barriers in the repository are also addressed.

The study is focussed on the repository design and waste inventory that was defined for the prestudy of SFL 3-5. Since the reporting of the prestudy the design of the repository has been modified and the waste inventory has been updated and a preliminary safety assessment of the repository has been carried out based on the new design and updated waste inventory. The implications on gas generation and release of these modifications in design and waste inventory are briefly addressed in this study.

Sammanfattning

Enligt nuvarande planer kommer långlivat låg- och medelaktivt avfall att deponeras i ett djupförvar, SFL 3-5. Den här studien omfattar beräkningar av hur mycket gas som kan bildas inne i avfallskollin och i de olika förvarsdelarna. Eventuell uppbyggnad av gastryck och den förträngning av vatten som detta kan innebära samt potentiella effekter på utsläppet av radionuklider från de tekniska barriärerna i förvaret belyses också.

Studien har i huvudsak genomförts för ett förvar med samma design och sammansättning på avfallet som i den tidigare utförda förstudien av SFL 3-5. Sedan genomförandet av förstudien så har förvarets design förändrats och en ny version av avfallets sammansättning tagits fram. Dessutom har en preliminär säkerhetsanalys genomförts för ett förvar med den nya designen och nya avfallssammansättningen. Påverkan på gas bildning och gasutsläpp av dessa förändringar i design och sammansättning på avfallet belyses översiktligt i denna rapport.

Summary

A deep repository, SFL 3-5, is presently planned for disposing of long-lived low- and intermediate-level waste. Detailed calculations of gas generation in SFL 3-5 by corrosion of metals in the repository and by microbial degradation of organic materials in the waste are made and the potential consequences of the gas generated are studied. These calculations are made for the repository design and waste inventory defined for the prestudy of SFL 3-5 that was reported in 1995 (Wiborgh (ed.), 1995). The issues addressed in the study are:

- gas pressure build-up and formation of volume expanding corrosion products which may affect the mechanical integrity of the repository barriers and thus the radionuclide release, and
- displacement of water in the repository barriers by gas and its influence on the transport and release of radionuclides.

The effects on the radionuclide release of replacing the bentonite and sand-bentonite barriers in SFL 3-5 with sand/gravel are also studied.

Based on the calculated gas pressure build-up inside the waste packages and in the concrete structure in SFL 3 it seems reasonable to assume that even if the concrete initially is gas tight, the internal gas pressure will cause cracks or open up slits through which gas may escape. This is to be expected within the first few tens of years after repository closure for the waste packages and within the first 200 years for the concrete structure. After this period, the barrier outside the concrete structure, i.e. bentonite and sand-bentonite or sand/gravel, will determine the gas escape. In case of sand-bentonite, the capillary pressure required for displacement of water and developing gas channels in sand-bentonite (about 50 kPa) has to be reached before gas can escape. Once this pressure is reached, only a small part of the porosity in the sand/bentonite is needed for gas to escape at the same rate as it is generated. In case of sand/gravel, gas escape will probably occur without major internal pressure build-up.

Gas escape from the waste contained in SFL 4 will probably occur without major internal pressure build-up. The maximum internal overpressure will most likely be determined by the resistance in the sand/gravel backfill and will probably not be higher than 0.1 to 1 kPa.

For SFL 5 it seems reasonable to assume that even if the waste packages and concrete structures are intact initially, the internal pressure build-up will create cracks or fractures. This will be initiated within 500 years of corrosion for the waste packages and within 1 000 years for the concrete structures. Once gas paths are created in the concrete structures only a small overpressure, 0.1 to 1 kPa , is needed for gas to escape through the sand/gravel backfill.

Some simple calculations of the radionuclide release from SFL 3 indicate that the maximum release rate of organic ^{14}C, ^{59}Ni, ^{129}I and ^{135}Cs from the near field not is affected by gas pressure build-up and displacement of water, but that displacement of water will lead to higher release rates at shorter times. In this aspect there is no difference between bentonite barriers and sand/gravel in SFL 3 for the cases studied. However, replacing the bentonite and sand/bentonite barriers with sand/gravel may result in higher maximum release rates of non-sorbing radionuclides with at most a factor of about 10. The effect on the release of other radionuclides depends on the

relation between their sorption capability in the different barrier materials and on their half-lives.

The preliminary safety assessment of SFL 3-5 is carried out for a design that is different from the design defined for the prestudy of SFL 3-5 and with a waste inventory that is updated since the prestudy. In addition, the repository depth is different in the preliminary safety assessment, 300 – 375 m, from that in the prestudy, 500 m. Rough estimates of the impact of these modifications in design and waste inventory give somewhat different results for gas generation and pressure build-up in SFL 3 and SFL 5, but the conclusions based on the earlier design and waste inventory are still valid. The results for SFL 4 are almost identical to the results for the old design and old waste inventory. The difference in repository depth has not been addressed in this study. A shallower location will result in larger gas volumes and faster pressure build-up, but this will not affect the main conclusions of this study.

Contents

1 Introduction

1.1 Background and aim

A deep repository, SFL 3-5, is presently planned for disposing of long-lived, low and intermediate level waste. The SFL 3-5 repository consists of three repository parts that will be used for different categories of waste. SFL 3 is intended for long-lived or toxic waste from Studsvik, and low- and intermediate level waste from CLAB and the encapsulation plant (EP). SFL 4 is intended for the fuel storage canisters from CLAB, for the decommissioning waste from CLAB and the encapsulation plant, and for the transport casks and transport containers. SFL 5 is intended for core components and internal parts from the nuclear power reactors.

A first preliminary and simplified assessment of the near-field as a barrier to radionuclide dispersion from the SFL 3-5 repository has been made within a prestudy of the SFL 3-5 repository concept (Wiborgh (ed.), 1995). One of the simplifications made in the prestudy was that potential effects of gas generation in the repository on the radionuclide release were neglected.

After closure and saturation of the SFL 3-5 repository gas can be generated. The main types of gas forming processes are:

- corrosion of steel and other metals in the waste and engineered barriers,
- microbial degradation of organic materials in the repository, and
- radiolytic decomposition of water caused by decaying radionuclides in the waste.

Some first estimates of the gas generation in the waste packages by these processes were made during the prestudy of the SFL 3-5 concept (Wiborgh (ed.), 1995). These estimates indicated that corrosion of metals in the waste packages dominates the gas generation, and that gas formed by radiolytic decomposition of water is negligible small. Gas formed by microbial degradation of organics in the waste may to some extent contribute to the gas formation rate in the waste packages in SFL 3.

The aim of the present study was to make more detailed calculations of gas generation by corrosion of metals in the repository, and to estimate the potential consequences of metal corrosion and gas generation in SFL 3-5 on the radionuclide release from the near-field barriers. There are several aspects of these processes that may affect the long-term behaviour of the near-field barriers in the repository and the radionuclide transport through the barriers. The issues addressed in this report are:

- gas pressure build-up and formation of volume expanding corrosion products, which may affect the mechanical integrity of the repository barriers and thus the radionuclide release, and
- displacement of water in the repository barriers by gas, which may affect the transport and release of radionuclides.

The original premises for this study were an SFL 3-5 repository with the same design as in the prestudy and located at a depth of about 500 metres in typical Swedish bedrock. As a result of the prestudy the option of replacing the bentonite barriers in SFL 3 with a

sand/gravel backfill became of interest. Therefore is was decided to also investigate the effects on the near-field release of radionuclides of replacing the bentonite barriers in SFL 3 with a sand/gravel backfill, still assuming the same design for the remaining part of the repository. However, before the conclusion of this study a new design of the SFL 3-5 repository was proposed and an update of the waste characterisation was finalised. In addition, it was decided to carry out a preliminary safety analysis of the repository concept based on the new proposed design, the updated waste inventory and utilising site-specific data derived for the safety assessment of the deep repository for spent fuel, SR 97. The influence of these new premises defined for the preliminary safety analysis of SFL 3-5 on gas generation, pressure build-up and gas escape are briefly addressed in this report (see Chapter 7), but the study is mainly built on the original premises.

2 Repository design

This chapter gives an overview of the SFL 3-5 design and estimated material volumes, voids, and amounts of corroding materials in the barriers, excluding the waste packages. This information is given as a background to the descriptions of gas generation and pressure build-up in Chapter 5. The design concept used in this study is the same as the concept used in the prestudy of the SFL 3-5 repository. This concept is based on the preliminary deep repository design given in (PLAN93).

2.1 SFL 3

In the applied design concept, the SFL 3 vault is about 80 m long, 15 m wide and 18 m high (Figure 2-1). The walls of the vault are covered with shotcrete. In the bottom of the vault a 0.1 m thick concrete plate is cast above a 0.3 m thick drainage layer of gravel. Above the concrete plate a 1.5 m thick bed of 90/10 sand/bentonite mixture is placed, on which a concrete structure is built. The waste containers/moulds are stacked in squared concrete cells, 2.5×2.5 m, and the remaining empty space in the cells is filled with porous concrete. The slot between the concrete cells and the rock, in average 1 m, is filled up with bentonite. A lid of concrete elements is placed on top of the concrete cells. A thin layer of sand, about 0.1 m thick, and a 1.5 m thick layer of 85/15 sand/bentonite covers the lid. A supporting concrete plate, about 0.1 m thick, is placed on top of the sand/bentonite and the remaining space is filled with gravel or sand.

The volumes of the different barriers and their thickness have been estimated by (Lindgren and Pers, 1994) and are summarised in Table 2-1. The estimated amount of reinforcement bars in the concrete structures is also given in Table 2-1. These estimates are based on the assumption of 100 kg reinforcement bars per m^3 of concrete. In addition, the estimated void in the barriers is given in Table 2-1, since this property is of importance to gas pressure build-up and displacement of water by gas. The voids are calculated by assuming the following porosity in the different materials (Wiborgh (ed.), 1995):

- 15% in concrete in the structures,
- 30% in the porous concrete,
- 60% in uncompacted bentonite,
- 25% in 90/10 sand/bentonite, and
- 53% in 85/15 sand/bentonite.

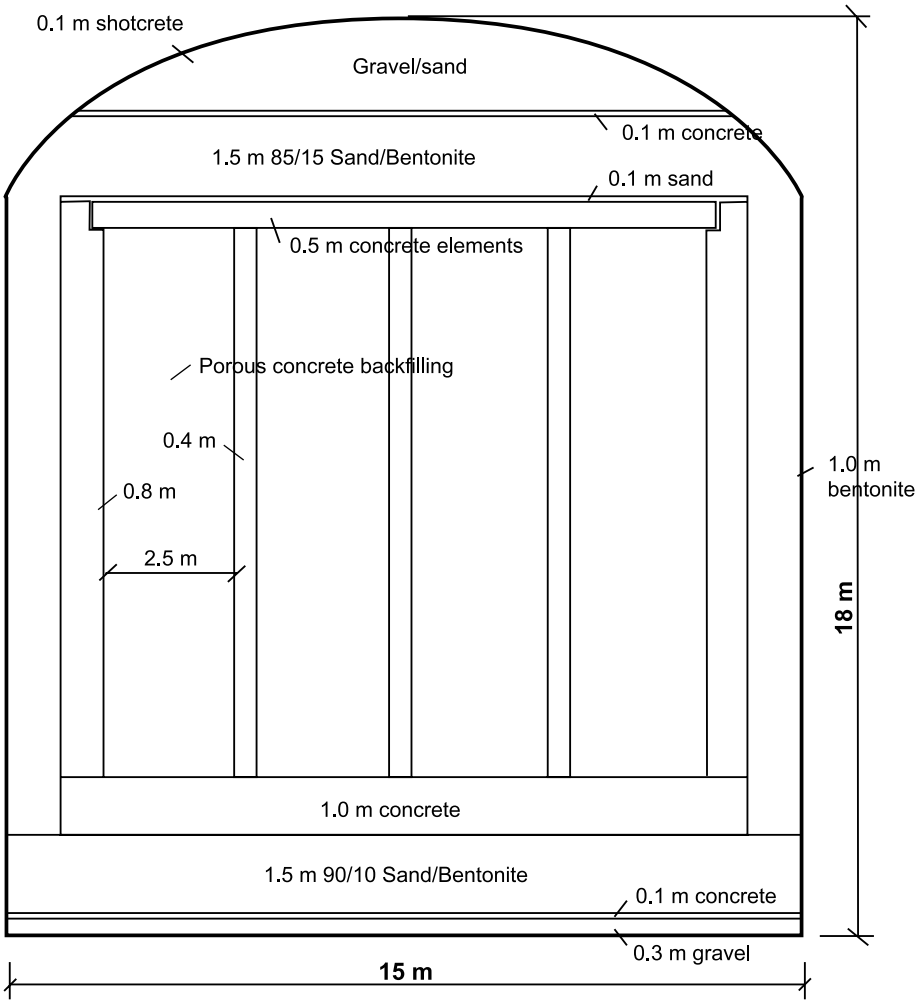

Figure 2-1 Schematic illustration of the SFL 3 design.

Table 2-1 Summary of estimated volumes, thickness, voids and amount of reinforcement bars in the barriers in SFL 3.

Barrier	Volume, [m^3]	Thickness, [m]	Void, [m^3]	Reinforcement, Fe [kg]
Concrete structures	*5 661*		*849*	*566 100*
side walls	1 577	0.8	237	157 700
bottom	921		138	92 100
top	461	0.5	69	46 100
internal walls	2 702	0.4	405	270 200
Porous concrete	*2 074*		*622*	
Bentonite (sides)	*2 025*	*1.0*	*1 215*	
Sand/bentonite	*3 760*		*1 466*	
90/10, bottom	1 880	1.5	470	
85/15, top	1 880	1.5	996	

An alternative design of the SFL 3, which have been discussed, is to replace the bentonite barriers with a sand/gravel backfill. In this case, the entire slot between the rock and the concrete walls, bottom and lid, in the vault would be filled with sand or gravel. Assuming a porosity of 30% for the sand or gravel backfill would change the void from 1 215+1 466 = 2 681 m^3 to (2 025 + 3 760)*0.3 = 1 736 m^3. Replacing the bentonite barriers with sand/gravel will not affect the gas generation rates and volumes, but the consequences of gas generation may be different. Therefore, in estimating these consequences, both design alternatives are considered (see Chapter 6).

2.2 SFL 4

The applied design concept for SFL 4 is shown in Figure 2-2. SFL 4 consist of the tunnel system remaining after deposition in SFL 3 and SFL 5 is concluded. The total length of the SFL 4 tunnel is about 500 m. The main part of the tunnel is 8.4 m wide and 5 m high. The walls are covered with shotcrete, and a 0.3 m thick concrete floor is cast above a 0.3 m thick drainage layer of gravel in the bottom of the tunnel. After placing the waste in the tunnel, the remaining space is backfilled with sand or gravel.

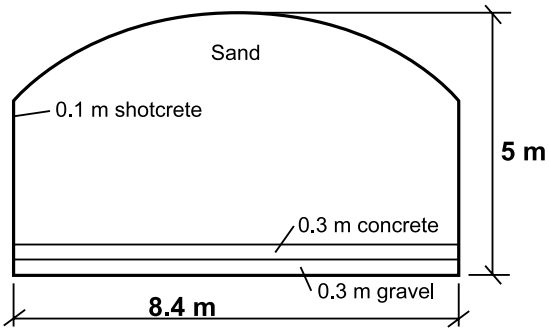

Figure 2-2 Schematic illustration of the SFL 4 design.

The volume and thickness of the sand/gravel backfill (Lindgren and Pers, 1994), and the void in the backfill assuming a porosity of 30% are as follows:

Volume = 10 770 m^3

Thickness = 1 m

Void = 3 231 m^3

In the applied design concept, SFL 4 does not contain any concrete structures with reinforcements or any other corroding metals, except the waste packages. These are described in Chapter 3.

2.3 SFL 5

In the applied design concept, SFL 5 consists of three vaults, each 130 m long, 7 m wide and 10.5 m high (Figure 2-3). A concrete floor is cast on top of a 0.3 m thick drainage layer of gravel. Reinforced concrete walls are placed on the concrete floor to form

compartments, ten in each vault. After piling the waste packages in the compartments, a 0.3 m thick lid of concrete elements is placed on the top of the compartments, and the remaining void in the vault outside the concrete compartments is backfilled with sand or gravel.

The estimated volume and thickness of the different barriers in the three SFL 5 vaults are given in Table 2-2, as well as the estimated void in the different barriers and the estimated amount of reinforcement bars in the concrete structures. The voids in concrete structures and in sand/gravel backfill are calculated assuming a porosity of 15 and 30%, respectively. The amount of reinforcements is calculated assuming 100 kg Fe per m^3 of concrete.

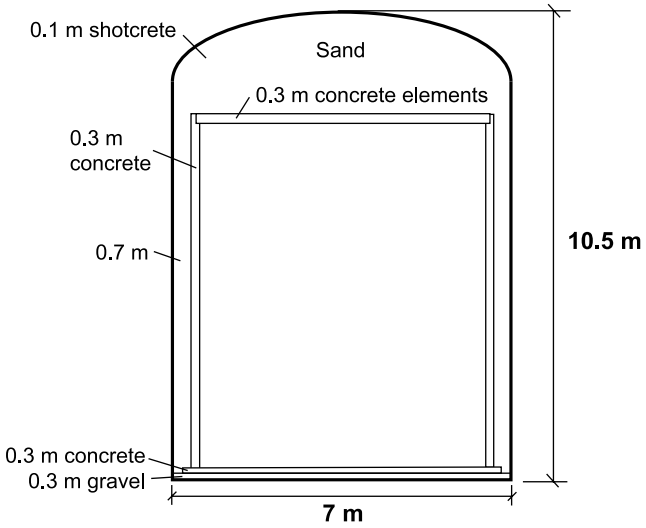

Figure 2-3 Schematic illustration of the SFL 5 design concept.

Table 2-2 Summary of estimated volumes, thickness, voids and amount of reinforcement bars in the barriers in the three SFL 5 vaults.

Barrier	Volume, [m^3]	Thickness, [m]	Void, [m^3]	Reinforcement, Fe [kg]
Concrete structures	*3 421*		*513*	*342 100*
long side walls	1 638	0.3	246	163 800
short side walls	126	0.5	19	12 600
bottom	702	0.3	105	70 200
lid	643	0.3	96	64 300
internal walls	312	0.3	47	31 200
Internal void, compartments	*3 408*		*3 408*	
Sand/gravel backfill	*10 920*	*0.7*	*3 276*	

3 Waste packages

In this chapter the waste packages allocated to the different repository parts are described, focussing on materials in waste and packaging that may generate gas and on voids in waste and packaging that may be accessible to the gas generated. The waste package descriptions are based on information derived in the waste characterisation study (Lindgren *et al.*, 1994) carried out as a part of the prestudy of the SFL 3-5 repository (Wiborgh (ed.), 1995).

3.1 SFL 3

Several different types of packaging will be used for the waste to be stored in SFL 3. The different types of packaging used for waste from Studsvik are:

- concrete containers with inner steel drums for unconditioned waste,
- steel drums for conditioned waste,
- steel drums with inner drums/cages for unconditioned waste,
- steel containers for unconditioned waste, and
- concrete boxes for conditioned waste.

The waste from CLAB and the Encapsulation plant will be packed in concrete boxes, cement solidified ion-exchange resins in boxes with expansion cassette and mixer, and concrete conditioned scrap in boxes with a steel grid.

These different packaging types and the waste that they will contain are briefly described below in terms of properties important for corrosion and gas generation. The estimated void and amount of metals that may generate gas during corrosion in packaging and waste are summarised in Table 3-1, as well as the amount of organic material in the waste, which by microbial degradation can contribute to gas formation. More detailed information on dimensions and amounts of gas generating materials is found in Tables 1 to 9 in Appendix A.

Concrete containers with inner steel drums

Concrete containers will be used for unconditioned intermediate level waste (Cont ILW), plutonium waste (Cont Pu) and tritium waste (Cont T). The containers are cubical with a side length of 1.2 m, and reinforced. Each container has five 105 litre holes prepared for 85 litre steel drums. The intermediate level waste is packed in these steel drums, while the plutonium and tritium waste first is packed in a steel container before placed in the steel drum. The voids are calculated assuming that 50% of the drums/containers are filled with waste, and that the porosity of the concrete is 15%.

Steel drums with conditioned waste

Liquid waste from the facilities in Studsvik (drum sludge) and decommissioning solutions (drum dec) will be treated to produce precipitates of iron(II)-hydroxide copper(II)-iron-cyanide. The sludge is conditioned with cement in steel drums with

mixers. The drum has an outer diameter of 0.57 m and a height of 0.84 m, and the thickness of the material is 0.0015 m. The void in the cement-conditioned waste is estimated assuming a porosity of 40%.

Steel drums with inner drums/cages

Steel drums with inner drums/cages are used for unconditioned ashes containing uranium (U-ashes), refuse and scrap containing plutonium (drum Pu), and refuse and scrap containing uranium and thorium (drum U+Th). The waste is placed in the inner drums/reinforcement cages and the space between the inner drums/cages and the outer drums are filled with concrete. The volumes of the inner and outer drums are 100 and 200 litres, respectively. The voids are calculated assuming that 50% of the inner drums/cages are filled with waste, and that the porosity of the concrete between inner drums/cages and outer drums is 15%.

Steel containers

Steel containers are used as packaging for cadmium, aluminium and iron scrap (St cont Cd) from decommissioning of the R1-reactor and for an ion-exchange cartridge (St cont dec) from decommissioning of facilities at Studsvik. The containers have the dimensions $1.2 \times 0.8 \times 0.8$ m. The voids are calculated assuming that 50% of the containers are filled with waste.

Concrete boxes

Concrete boxes are used as packaging for plutonium contaminated glove boxes from Studsvik (Cont box Pu) and for operational waste from CLAB and the Encapsulation plant, ion-exchange resins from the clean-up system (CLAB/EP resin) and scrap and trash (CLAB/EP scrap).

The concrete boxes with glove boxes have the dimensions $1.4 \times 1.3 \times 1.1$ m, and are made by pouring concrete around the glove boxes. The concrete boxes for operational waste from CLAB and the Encapsulation plant are reinforced and cubical with a side length of 1.2 m and a wall thickness of 0.1 m. The boxes for cement-conditioned ion-exchange resins are equipped with a 0.02 m thick expansion cassette of polyurethane foam plastics, a steel stirrer and a steel lid. The boxes for scrap and trash stabilised in concrete are equipped with a special steel grid used to compact the waste in the box and to prevent pieces of waste from floating when concrete is poured.

The void in the packages with glove boxes is estimated by assuming a porosity of 40% for the whole package. The void in the packages with ion-exchange resins and scrap is estimated by assuming a porosity of 40% for the conditioned waste and 15% for the concrete box.

Table 3-1 Summary of estimated void and amount of gas generating metals and organic materials in waste packages in SFL 3.

Waste package	No of packages	Void, [m^3]	Metals, [tonnes]		Organics, [tonnes]	
			Fe	Al	Cellulose	Other
Concrete containers with inner steel drums						
Cont. ILW	400	157	174	32	0.8	2
Cont Pu	100	39	49	3	0.7	4.5
Cont T	2	0.8	0.8			
Steel drums with conditioned waste						
drum sludge	600	51	36			0.3
drum dec	100	8.6	6			0.05
Steel drums with inner drums/cages						
U-ashes	147	9.6	5			
drum Pu	400	26	40	4	2	2
drum U+Th	1 000	65	100	10	5	5
Steel containers						
St cont Cd	12	4.6	2	1		
St cont dec	1	0.4	1			0.1
Concrete boxes						
Cont box Pu	29	23	2			0.3
CLAB/EP resin	1 800	917	468			270
CLAB/EP scrap	360	183	103	1	37	56
Total	**4 951**	**1 485**	**987**	**51**	**46**	**340**

Total amount of gas generating materials

The total estimated amount of metals and organic materials in waste and packaging in SFL 3 is given in Table 3-2. The waste packages contain almost 990 tonnes of steel material, of which about 80% is packaging materials. The waste category 'CLAB/EP resin' contributes with almost 50% of the total amount of steel materials, despite that there is no steel in the waste in this category. The waste category 'drum U+Th' has the largest amount of steel materials in the waste, and the waste category 'Cont ILW' has the largest amount of aluminium in the waste. The operational waste from CLAB and the encapsulation plant contributes with most of the organic materials. Excluding cellulose, these two waste categories contain 96% of the total amount of organic materials, 79% in 'CLAB/EP resin' and 17% in 'CLAB/EP scrap'. The waste category 'CLAB/EP scrap' also contains about 80% of the total amount of cellulose in the waste packages in SFL 3. The total estimated void in the waste packages in SFL 3 is about 1 500 m^3.

Table 3-2 Total amount of metals and organic materials in SFL 3 waste packages [tonnes].

	Fe	Al	Cellulose	Organics
Waste	217	51	46	340
Packaging	770			
Total	987	51	46	340

3.2 SFL 4

The packaging proposed for SFL 4 waste is a cubic carbon steel vessel with a side length of 2.4 m, a wall thickness of 6 mm, a weight of 1 600 kg, and an inner volume of 13.6 m^3. The different waste types that will be packed in these cubic steel vessels are:

- decommissioning waste from CLAB, and
- decommissioning waste from the encapsulation plant.

Another waste type that may be allocated to SFL 4 contains transport casks and containers. These casks and containers will probably be deposited without any further packaging or shielding.

The estimated void in waste and packaging and the amount of metals that may generate gas during corrosion in packaging and waste are summarised in Table 3-3. More detailed information on amounts and dimensions is given in Table 10 in Appendix A. The waste allocated to SFL 4 will not contain any organic materials, since organic materials such as shock-absorbers and neutron shielding in transport casks will be removed before disposal.

The decommissioning waste from CLAB is divided into three waste categories: steel components (Steel CLAB*)*, concrete (Concr. CLAB*)*, and fuel storage canisters (Can. CLAB*)*. The decommissioning waste from the encapsulation plant is divided into two waste categories: steel components (Steel EP) and concrete (Concr. EP).

The waste category ‘Steel CLAB’ mainly contains parts from the cooling and clean-up system in the storage pool. The waste category ‘Steel EP’ contains similar types of steel components. The void inside the waste packages is estimated based on the assumption of a filling degree of 35%.

The waste category ‘Concr. CLAB’ contains concrete chipped off from the buildings, and so does the waste category ‘Concr. EP’. The waste itself does not contain any steel. The void inside the waste packages is estimated based on the assumption of a filling degree of 50%.

The waste category ‘Can. CLAB’ consists of fuel storage canisters that will be cut and packed in the steel vessels. The void inside the waste packages is estimated from the weight and density of the storage canisters and the assumptions that nine half canisters will be placed in each steel vessel.

The waste categories*,* ‘Casks fuel’ ‘Casks core’, ‘Casks can.’ and ‘Cont. ILW’ contains casks and containers used for transportation. The void estimated for each of these waste categories is based on the assumption that the casks and containers will not be compacted or backfilled before disposal.

The total amount of steel in waste and packaging in SFL 4 is estimated to be about 10 000 tonnes, of which about 1 000 tonnes is the steel packaging. The waste categories ‘Steel CLAB’ and ‘Can. CLAB’ have the largest amounts of steel in the waste, about 2 500 and 3 200 tonnes, respectively. Including also the steel in the packaging, these waste categories together contribute with 67% of the total amount of steel in SFL 4, ‘Steel CLAB’ with 27% and ‘Can. CLAB’ with 40%.

The total estimated void in waste packages and in transport casks and containers is about 8 400 m^3, of which 83% is the void in the waste categories which also have the largest amount of steel namely 'Can. CLAB' with 73% and 'Steel CLAB' with 10% of the total void.

Table 3-3 Summary of estimated void and amount of steel in waste packages in SFL 4.

Waste package	No of packages	Void [m^3]	Steel [tonnes]
Cubic carbon steel vessels			
Steel CLAB	98	867	2 657
Concr. CLAB	53	361	85
Can. CLAB	480	6 118	3 968
Steel EP	6	53	163
Concr. EP	3	20	5
No packaging			
Casks fuel	10	66	540
Casks core	2	13	108
Casks can.	40	320	1 240
Cont. ILW	25	590	1 289
Total	**717**	**8 408**	**10 055**

3.3 SFL 5

The packaging that is proposed for SFL 5 waste is a reinforced concrete container with an inner steel cassette. The outer dimensions of the container are $1.2 \times 1.2 \times 4.8$ m, and the wall thickness is 0.1 m. The inner volume of the container is 4.6 m^3. The waste is placed in the steel cassette in the container and the container is backfilled with concrete. The outer and inner volumes of the steel cassette are 2.5 and 2 m^3, respectively.

The different waste types that will be packed in these concrete containers are:

- core components and internal parts from BWR reactors,
- core components and internal parts from PWR reactors, and
- some metal parts from the R2 reactor in Studsvik.

The estimated void in waste and packaging and the amount of metals, which may generate gas during corrosion in packaging and waste, are summarised in Table 3-4. The waste allocated to SFL 5 will not contain any organic materials. More detailed information on volumes, amounts and dimensions is given in Tables 11 and 12 in Appendix A. The void in the packaging is estimated assuming that the porosity in the concrete container walls is 15%, and that the total volume outside the steel cassette and half of the volume inside the cassette is backfilled with concrete with a porosity of 30%. The void in the waste package is the void in the packaging minus the estimated waste volume.

Table 3-4 Summary of estimated void and amount of gas generating metals in waste packages in SFL 5.

Waste category	No of packages	Void, [m^3] Total	Void, [m^3] Inside cassette	Steel [tonnes]	Zircalloy [tonnes]
BWR					
Grid	128	270	155	214	
Tank	81	143	67	363	
Tank cover	189	370	200	525	
Core spray	108	228	131	177	
Contr. rod tubes	45	90	49	117	
Instr. tubes	9	19	11	11	
Boron plates	20	42	24	36	
Contr. rods	419	872	494	764	
Used parts	4	8	5	5	2
Box-fuel channels	14	29	16	13	13
Box-tran. pcs	1	2	1	3	
Box+detect.	11	23	13	11	7
Box+PRM sonds	12	25	14	14	8
PRM sonds	57	124	73	62	
TIP detect.	19	31	14	18	
PWR					
Tank	63	111	54	280	
Rod bundles	51	111	65	49	
Internal parts	150	288	153	470	
Studsvik					
Reactor parts	1	2	1	1	
Total	**1 382**	**2 788**	**1 534**	**3 133**	**30**

The total amount of steel in the waste packages in SFL 5 is estimated to be about 3 130 tonnes, of which about 1 860 tonnes is in the waste. The steel cassettes contribute with about 830 tonnes and the reinforcements in the concrete containers with about 440 tonnes. The estimated total amount of Zircalloy is almost 30 tonnes. The total void in the waste packages is estimated to be about 2 800 m^3, of which about 55% is the void inside the steel cassettes.

4 Gas generation processes

Gas can be generated in the repository by hydrogen evolving corrosion of metals in SFL 3-5 and by microbial degradation of organic materials in SFL 3. Gas may also be formed by radiolytic decomposition of water, but in the prestudy of the SFL 3-5 concept (Wiborgh (ed.), 1995) it was shown that this process gives a negligible small contribution to the gas generation. In this chapter the assumptions, equations and data used to estimate gas generation by corrosion of metals and by degradation of organics are given.

4.1 Corrosion

Steel is the major metal present in the repository, but the waste also contains other metals such as aluminium, Zircalloy, Inconel, lead, cadmium, brass, copper and beryllium. In addition to steel, only aluminium and Zircalloy are considered as gas generating materials in SFL 3-5. The remaining metals are either thermodynamically stable at the conditions expected or is present in such small amounts that their contribution to the gas generation in the repository is negligible.

Steel is present in all repository parts. Hydrogen evolving corrosion of steel can occur only in the absence of dissolved oxygen. That implies that anaerobic corrosion will start when aerobic corrosion or some other oxygen consuming reaction, such as microbial activity has consumed the oxygen initially present.

When anaerobic conditions prevail, the amount of hydrogen evolved can be estimated by the following overall reaction for corrosion of steel, for which the formation of magnetite is the end product (Höglund and Bengtsson, 1991).

$$3\ Fe(s) + 4\ H_2O \rightarrow Fe_3O_4(s) + 4\ H_2(g)$$

Aluminium is present in the waste in SFL 3. Due to the large amount of concrete in SFL 3, the water in contact with the aluminium waste will be alkaline. Aluminium is not thermodynamically stable in water, but has a very dense protective oxide layer. However, in alkaline environments this oxide layer will dissolve and a rapid corrosion of aluminium yielding hydrogen can take place according to the reaction (Höglund and Bengtsson, 1991):

$$2\ Al(s) + 2\ OH^- + 4\ H_2O \rightarrow 2\ AlO(OH)_2^- + 3\ H_2(g)$$

or alternatively

$$2\ Al(s) + 2\ OH^- + 2\ H_2O \rightarrow 2\ AlO_2^- + 3\ H_2(g)$$

Zircalloy is present in the waste in SFL 5, and will be exposed to water with elevated pH. Zircalloy is an alloy with approximately 98% zirconium. Anaerobic corrosion of zirconium can occur according to the following reaction:

$$Zr(s) + 2\ H_2O \rightarrow ZrO_2(s) + 2\ H_2(g)$$

However, the formation of zirconium oxide will passivate the surface, and the corrosion rate of Zircalloy is therefore very low.

In calculating the gas formation rates due to corrosion it is assumed that all corroding metal parts, except reinforcements in concrete packages and concrete structures, have a planar geometry. The gas formation rate due to corrosion of a slab (i.e. plates where corrosion of the ends is disregarded) can be expressed as:

$$G = A \cdot r \cdot \rho \cdot \frac{1}{M_V} \cdot X \cdot V_0 \qquad (4\text{-}1)$$

where:

G	is the gas generation rate (m^3(STP)/year)
A	is the surface area (m^2)
r	is the corrosion rate (m/yr)
ρ	is the density of the metal (kg/m^3)
M_V	is the weight per mole of metal (kg/kmole)
X	is the stoechiometric coefficient (kmole H_2/kmol metal)
V_0	is the molar volume of ideal gas at 0ºC and 1 atm = 22.4136 m^3 (STP)/kmole gas.

Gas generation by corrosion of reinforcement bars considering the shrinking surface can also be described by equation 4-1 with the difference that the corroding surface area A is a function of time according to:

$$A(t) = 2 \cdot \pi \cdot R(t) \cdot L \qquad (4\text{-}2)$$

where

$$R(t) = R_0 - r \cdot t \qquad (4\text{-}3)$$

and

$$L = \frac{m}{\rho \cdot \pi \cdot R_0^2} \qquad (4\text{-}4)$$

and

R	is the radius of the reinforcement bars at time t (m)
R_0	is the initial radius of the reinforcement bars (m)
t	is the time (years)
L	is the length of the reinforcement bars (m)
m	is the weight of the reinforcement bars (kg).

The metal specific data used in the calculations of the gas generation rates are given below.

Steel: $r = 10^{-6}$ m/year (Lindgren and Pers, 1994)
$\rho = 7\ 800$ kg/m^3
$M_V = 55.847$ kg/kmole
$X = 4/3$ kmole H_2/kmol Fe

Zircalloy: $r = 10^{-8}$ m/year (Lindgren and Pers, 1994)
$\rho = 6\ 500$ kg/m^3
$M_V = 91.22$ kg/kmole
$X = 2$ kmole H_2/kmol Zr

Aluminium: $r = 10^{-3}$ m/year (Lindgren and Pers, 1994)
$\rho = 2\ 700$ kg/m^3
$M_V = 26.9815$ kg/kmole
$X = 3/2$ kmole H_2/kmol Al

4.2 Microbial degradation

Organic materials are present in the waste in SFL 3. These materials may be digested by micro-organisms, which can generate gases. The chemical environment significantly influences the rate of microbial degradation, where optimal conditions for most micro-organisms are a pH close to neutral, a temperature of 25 – 30ºC, and absence of bio-toxic substances. However, different micro-organisms do possess a remarkable ability to adapt to different environments. Therefore, microbial activity and gas generation cannot be excluded even if strongly alkaline conditions are expected in the SFL 3 waste packages after saturation of the repository.

Under aerobic conditions, microbial degradation of organics will consume oxygen and produce carbon dioxide. Because of this process and because of aerobic corrosion of the large amounts of steel in the repository it is assumed that the rather small amounts of oxygen initially present after repository closure quickly will be consumed to establish anaerobic conditions in the repository.

Under anaerobic conditions, other oxidants such as nitrate, sulphate and carbon dioxide will participate in the microbial degradation process. A simplified reaction formula for the degradation of an arbitrary organic compound could be written as (Höglund and Bengtsson, 1991):

C_{org} + Oxidant → C^*_{org} + H_2 + CO_2 + CH_4 + Reducing agent

Gas generation rates for microbial degradation of organic materials are relatively sparse. The type of organic substrate as well as the surface area available for microbial attack is important for the degradation rate.

In estimating the gas generation from microbial degradation of organics in SFL 3 waste, the organic material was divided into two groups, cellulose materials with a large surface to volume ratio and other organic materials with a low surface to volume ratio. The latter group includes ion exchange resins, plastics, rubber etc. The gas generation rates (Wiborgh *et al.*, 1986) and maximum yields (Brandberg and Wiborgh, 1982) assumed for these two groups of organic materials are given below.

	Cellulose	**Other organics**
Rate (mole gas/year, kg organic)	0.7	0.05
Maximum yield (mole gas/kg organic)	37	30

The relative proportions between soluble (CO_2) and insoluble (CH_4 and H_2) gases formed are dependent on the chemical environment. In this study it is assumed that equal amounts of soluble and insoluble gases are generated (Wiborgh *et al.*, 1986).

5 Gas generation, pressure build-up and gas escape

In this chapter the estimated gas generation rates and volumes are given and resulting gas pressure build-up and gas escape from the repository are evaluated. The information given in the previous chapters is utilised in the calculations, i.e. the results are derived for the same repository design, repository location and waste type description that applied in the prestudy of SFL 3-5 (Wiborgh (ed.), 1995).

5.1 SFL 3

5.1.1 Gas generation rates and volumes

The estimated gas generation rates in SFL 3 from corrosion of metals in waste packages and concrete structures are given in Figure 5-1 and Table 5-1. Due to the fast corrosion of aluminium in the waste, the initial gas formation rate in SFL 3 waste is estimated to be almost 350 m^3/year at repository depth. Adding to this the gas generation from corrosion of packaging and reinforcement bars in the concrete structures will give a gas formation rate of 355 m^3/year (Figure 5-1, upper and Table 5-1). After 5 years when aluminium in the waste has corroded away, the gas formation rate decreases to about 6.5 m^3/year and is dominated by the corrosion of the steel packagings (Figure 5-1, lower). The contribution from corrosion of the steel packagings decreases stepwise with time as packagings with increasing thickness are consumed. After about 5 000 years of corrosion the dominating corroding material left is the reinforcement bars in concrete structures and concrete packaging. The gas generation rate at that time is about 1 m^3/year. After 8 000 years the reinforcement bars are consumed and the only corroding material left is the thick-walled inner containers in the waste category 'Cont. Pu', giving a gas generation rate of about 0.01 m^3/year. After 10 000 years no more gas generating metals are left in SFL 3.

The initial gas generation rate and the rate after 5 years when aluminium is consumed are shown for the different waste categories in Figure 1 in Appendix B. The waste category 'Cont. ILW' will initially generate gas at the highest rate, while the highest rate after 5 years is obtained for the waste category 'CLAB/EP resin'.

The gas formation rate due to microbial degradation of organics in the waste is shown in Figure 5-2. The estimated gas generation rate during the initial 50 years is 11 m^3/year at repository depth. After 50 years the rate decreases to about 4 m^3/year because the maximum yield for cellulose degradation is reached. Degradation of other organics will continue to generate gas at this rate during another 550 years before the maximum yield for this degradation is reached.

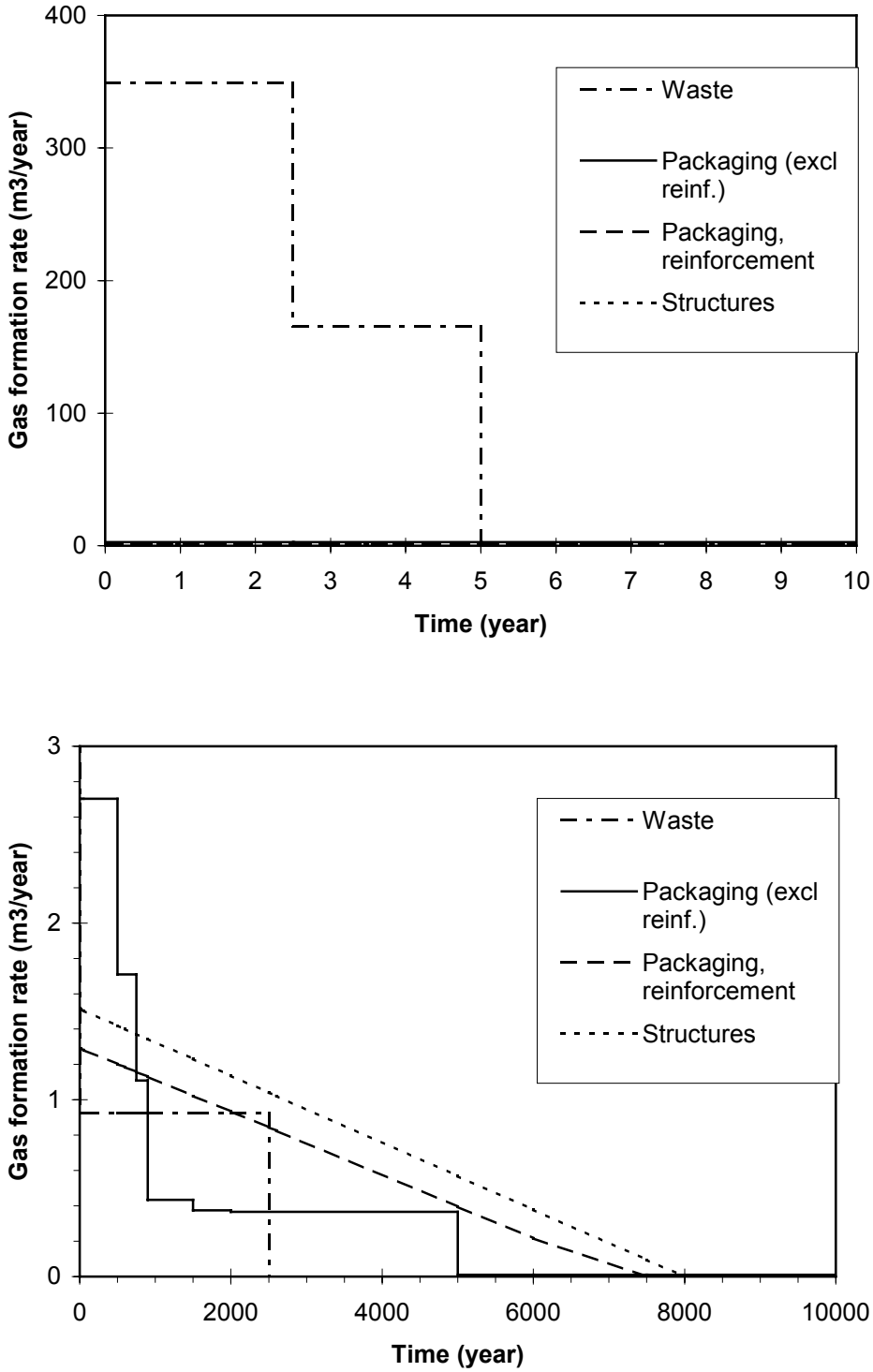

Figure 5-1 Gas formation rates at repository depth due to corrosion in SFL 3. Upper: 0 – 10 years. Lower: 0 – 9 000 years.

Table 5-1 Initial gas generation rates and maximum theoretical gas volume that can be generated at 500 m depth due to corrosion of metals in SFL 3.

	Initial gas generation rate, [m^3/year]	Maximum theoretical gas volume, [m^3]
Waste	**349**	**3 600**
Steel	0.9	2 320
Aluminium	348	1 280
Packaging	**4.0**	**8 240**
Reinforcement bars	1.3	4 700
Other steel materials	2.7	3 540
Concrete structures	**1.5**	**6 060**
Total	**355**	**17 900**

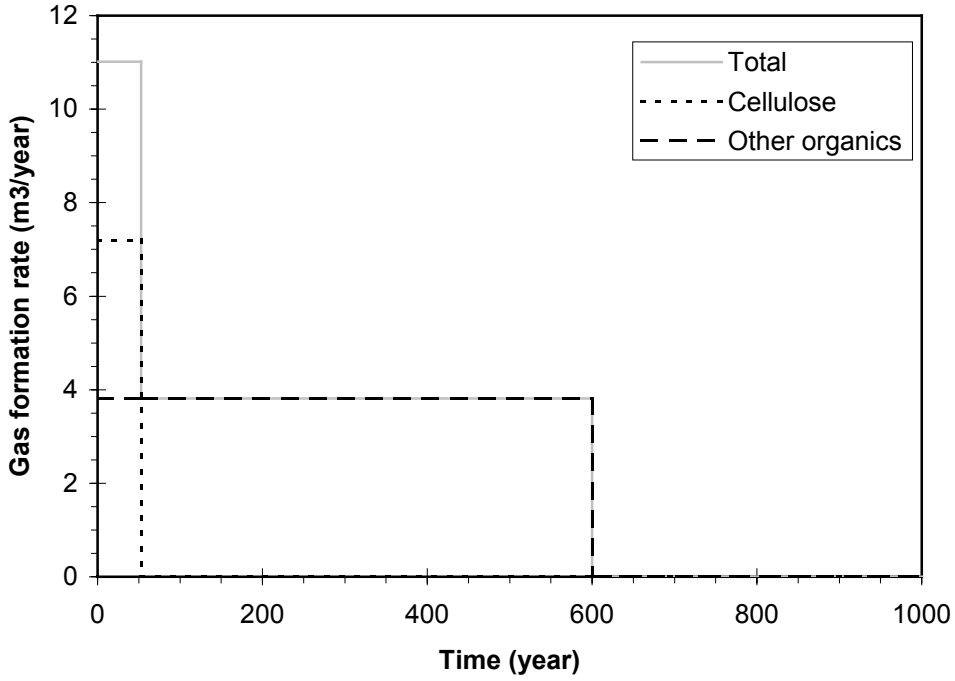

Figure 5-2 Insoluble gas formation rate at repository depth due to microbial degradation of organic materials in SFL 3.

Excluding the first 5 years, when aluminium corrosion dominates the gas generation rate in the waste packages, microbial degradation of organics will generate gas at a rate which is approximately twice as high as the gas generation rate due to corrosion of metals in the waste packages during the initial 50 years. From 50 years up to 600 years, the gas formation rates due to corrosion and due to microbial degradation of organics in the waste are of similar magnitude.

The rates of gas generation by all the waste, all the waste packages and the total gas generation rate inside the bentonite barriers as a function of time are depicted in separate graphs in Figure 5-3. Initially, the total gas generation rate due to corrosion and microbial

degradation of organics inside the bentonite barriers will be almost 370 m^3/year at repository depth. After 5 years when all aluminium in the waste has corroded away, the total gas generation rate will decrease to about 18 m^3/year. This rate will be maintained as long as there still is cellulose present in the waste. After 53 years when the maximum yield of cellulose degradation is reached, the rate decreases to about 10 m^3/year. The next larger decrease in gas generation rate occurs after 600 years when the maximum yield of degradation of other organics than cellulose is reached. From this time until year 5 000 the rate will decrease both continuous and stepwise from about 5 to 1 m^3/year.

The estimated volumes of gas formed by corrosion and microbial degradation in the different waste types in SFL 3 (waste and packaging) at repository depth are given in Tables 1 to 5 in Appendix B. The volumes given are for 1 and 5 years of corrosion and microbial degradation, as well as the maximum volume that theoretically may be generated. In addition, the time required generating a gas volume equal to the total void in waste and packaging is given in the tables. If gas cannot escape from the waste package, this is a measure of the time delay of gas pressure increase in the waste packages. However, it should be noted that a large part of the water in cement and concrete is capillary bound and cannot be expelled by gas. The void accessible to gas is therefore smaller than the total void in the waste packages containing cement or concrete.

In all waste types containing aluminium (‘Cont. ILW’, ‘Cont. Pu’, ‘drum Pu’, ‘drum U+Th’, ‘St cont Cd’) it will take less than a year to generate a gas volume that is equal to the void in the waste packages. This is of course due to the fast corrosion of aluminium. For the rest of the waste types from Studsvik (‘Cont T’, ‘drum sludge’, ‘drum dec’, ‘U-ashes’, ‘St cont dec’), except the concrete boxes with plutonium contaminated glove boxes (‘Cont box Pu’), a gas volume equal to the void in the waste packages will be generated in less than 100 years. In the concrete boxes with plutonium contaminated glove boxes (‘Cont box Pu’), the maximum volume of gas that theoretically can be generated will not exceed the void in the packages.

In the waste packages from CLAB/EP with scrap (‘CLAB/EP scrap’) and ion exchange resins (‘CLAB/EP resin’) it will take about 20 and 200 years, respectively, to generate a gas volume equal to the void in the packages. In these packages, microbial degradation of organics will give larger volumes of gas during the first five years than corrosion of metals in the waste and packaging.

The gas volume (at repository depth) generated by corrosion of metals in waste, packaging and concrete structures and by microbial degradation of organic materials in the waste are shown as a function of time in Figure 5-4. During the first hundred of years, corrosion of metals in the waste and microbial degradation in the waste will produce the largest volumes of gas. These gas sources will cease after about 2 500 and 600 years, respectively (see Figures 5-1 and 5-2). After about 1 000 years, corrosion of metals in packaging materials will have generated the largest volume of gas. Corrosion of packaging materials and of reinforcement in concrete structures will continue to generate gas for several thousands of years, but no more gas generation is expected after 10 000 years.

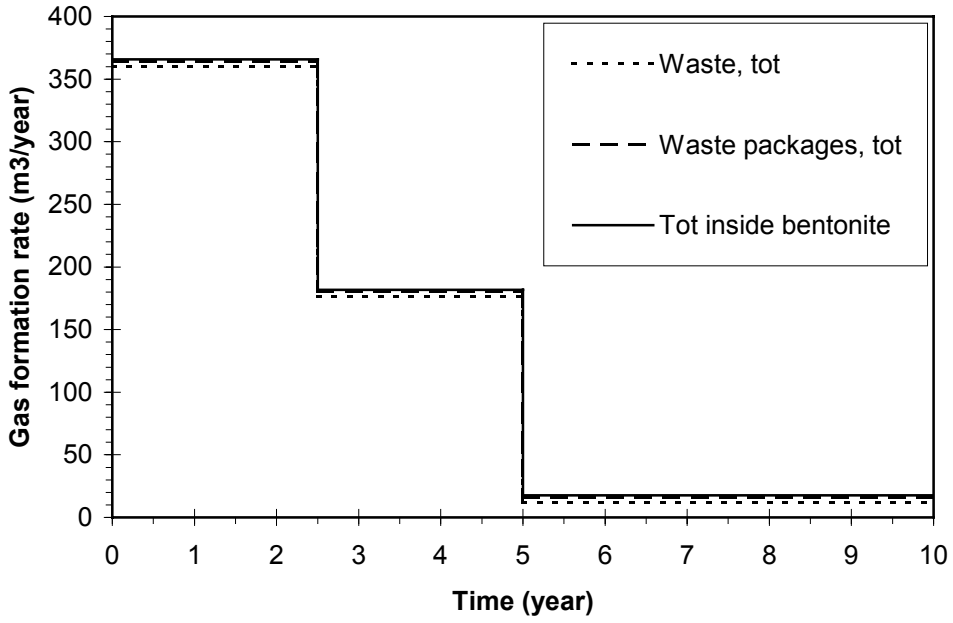

Figure 5-3 Gas generation rates as a function of time at repository depth in waste, waste packages and totally inside the bentonite barriers in SFL 3.

The amount of water required initially and to maintain hydrogen evolving corrosion at the assumed rates during the initial 5 years and over the whole time period when corrosion occurs has been calculated (see Appendix C). During the initial 5 years approximately 54 m^3 of water is required for corrosion of metals in the waste packages. This corresponds to about 4% of the water contained in the waste packages at full saturation. Approximately 580 m^3 of water is required to corrode away the total amount of metals in the waste packages, i.e. about 40% of the initial volume in the waste packages at full saturation. Consumption of all the reinforcement bars in the concrete structures by hydrogen evolving corrosion requires approximately 240 m^3 of water, i.e. about 50% of the water contained in the structures at full saturation.

5.1.2 Pressure build-up

If gas cannot escape through the barriers in SFL 3 at the same rate as it is generated, the gas pressure inside the barriers will start to increase when the void in the barriers accessible to gas is exceeded. The gas volumes generated in SFL 3 waste packages, concrete structures and in total after 1, 5 and 10 000 years (maximum theoretical volume) by microbial degradation of organics and by corrosion of metals are given in Table 5-2. In addition, the ratio between the gas volume and the void in the waste packages as well as between the total gas volume and the void in the interior of the SFL 3 (inside the bentonite barriers) are given. This ratio shows that the gas pressure inside the packages will start to increase during the first 5 years if gas accumulates in the packages and the void accessible to gas in the packages is less than 90% of the total void in the packages. An increase in gas pressure inside the bentonite barriers during the first 5 years could be expected if the void accessible to gas in waste packages, porous concrete and concrete structures is around 40% of the total void.

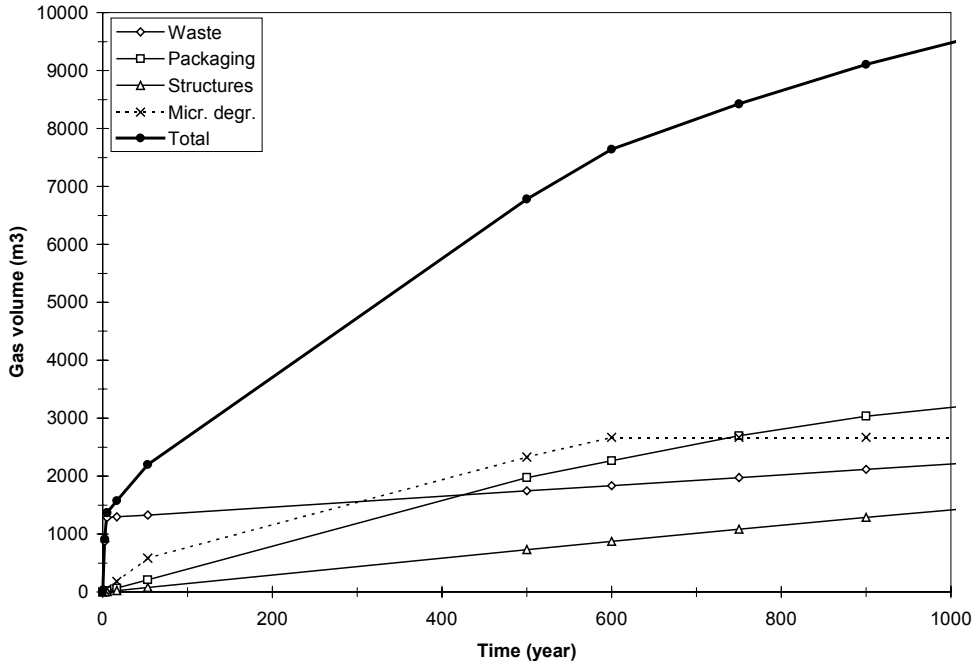

Figure 5-4 Gas volumes generated at repository depth by corrosion of metals in waste, in packaging and in concrete structures and by microbial degradation of organics in the waste in SFL 3.

Table 5-2 Volume of gas at repository depth after 1, 5 and 10 000 years of corrosion and microbial degradation in SFL 3 (maximum theoretical volume), and the ratio gas volume to void in waste packages and in concrete structures + porous concrete + waste packages.

Time, [years]	Gas volume, [m^3]			Ratio gas volume to void	
	Waste packages	Concrete structures	Total	Waste packages	Total inside bentonite
1	364	1.5	366	0.25	0.12
5	1 360	7.6	1 368	0.92	0.46
10 000	14 510	6 060	20 570	9.8	7.0

The pressure increase in the system inside the bentonite barriers in SFL 3 is shown in Figure 5-5 assuming that gas cannot escape through the bentonite barriers. Four curves are displayed in the figure. Two of the curves represents the assumption that the total void in the waste packages, the porous concrete surrounding the waste packages and the concrete structures is accessible to gas. The other two curves represents the assumption that the void accessible to gas is equal to the volume of free water in the system inside the bentonite barriers, i.e. the volume of water that is not strongly bound to the concrete materials by capillary forces. For each of these two assumptions the pressure build-up caused by all gas generated inside the bentonite barrier and by the gas generated in the waste packages only are shown.

The volume of free water is estimated using the same assumptions as were used for the silo in SFR (Moreno and Neretnieks, 1991). These assumptions are:

- In concrete structures and in concrete container walls the amount of free water is negligible since the capillary forces in normal structural concrete are very strong, of the order of 1 – 2 MPa.
- In porous concrete the amount of free water is 10% of the porosity.
- In cement conditioned waste the amount of free water is 30% of the porosity.
- In unconditioned waste the total void inside the waste packages is free water.

With these assumptions the volume of free water is estimated to be 535 m^3, of which 62 m^3 is free water in the porous concrete and the remaining 473 m^3 is free water inside the waste packages. The estimated free water volume is about 18% of the total void in the system inside the bentonite barriers.

Figure 5-5 shows that the internal gas pressure will exceed the hydrostatic pressure after about 150 years if the total internal void is accessible to gas, and within the first two years if only the volume of free water inside the bentonite barriers is accessible to gas. If gas continues to accumulate inside the bentonite barriers the internal pressure will increase, and after about 500 years an overpressure of about 5 MPa is reached if the total internal void is accessible to gas. If only the free water volume is accessible to gas, the overpressure after 500 years would be 50 – 60 MPa. During the first thousands of years the pressure build-up is totally dominated by gas generated by the waste packages, as is shown by the small difference between the curves for all gas and waste package gas in Figure 5-5.

These estimated overpressures are high compared to the gas pressure required to open up gas paths in the bentonite barriers and also higher than the design pressure of the concrete structures. The critical overpressure for gas escape through sand/bentonite and uncompacted bentonite used in the safety analysis of the silo in SFR was 50 kPa (Moreno and Neretnieks, 1991). The concrete structure in the silo in SFR is constructed for a maximum internal overpressure of 280 kPa (Moreno and Neretnieks, 1991), and the concrete structure in SFL 3 can withstand an external load of about 1 MPa (Harry Larsson, pers. com. 1995). These figures and the pressure build-up curves in Figure 5-5 suggest that a concrete structure that initially is intact enough to prevent gas escape will be exposed to such high internal gas pressures that cracking of the structures is to be expected within the first 200 years of gas generation. It should be noted that this time estimate is based on the assumption that gas generated inside the waste packages may escape out from the packages.

Figure 5-6 shows the gas pressure build-up inside the waste packages in SFL 3 assuming that gas cannot escape from the packages and that the total void or the volume of free water inside the packages is accessible to the gas generated inside the packages. Since some of the gas generated by the packaging material not is generated inside the packages, e.g. gas from external corrosion of steel containers, both the pressure build-up due to waste generated gas only and due to gas generated by waste and packaging are shown in the figure. These curves indicate that gas accumulation inside the waste packages will lead to an internal overpressure within the first 20 years of gas generation, and after 50 years the overpressure will exceed 1 MPa. If the internal void accessible to gas is equal to the estimated volume of free water, an internal overpressure of almost 10 MPa will be reached within the first 5 years. Based on these calculated overpressures it seems reasonable to assume that even if the waste packages initially are gas tight, the internal gas pressure will

cause cracks or open up slits through which the gas may escape, and that this may occur within the first few tens of years after repository closure.

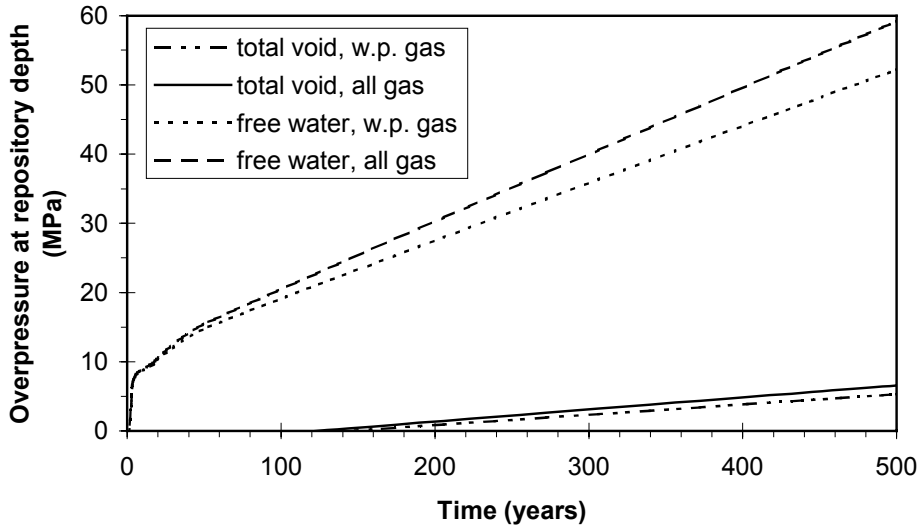

Figure 5-5 Overpressure inside the bentonite barriers in SFL 3 at repository depth as a function of time due to gas generated by the waste packages (w.p. gas) and due to all gas generated inside the bentonite barriers (all gas).

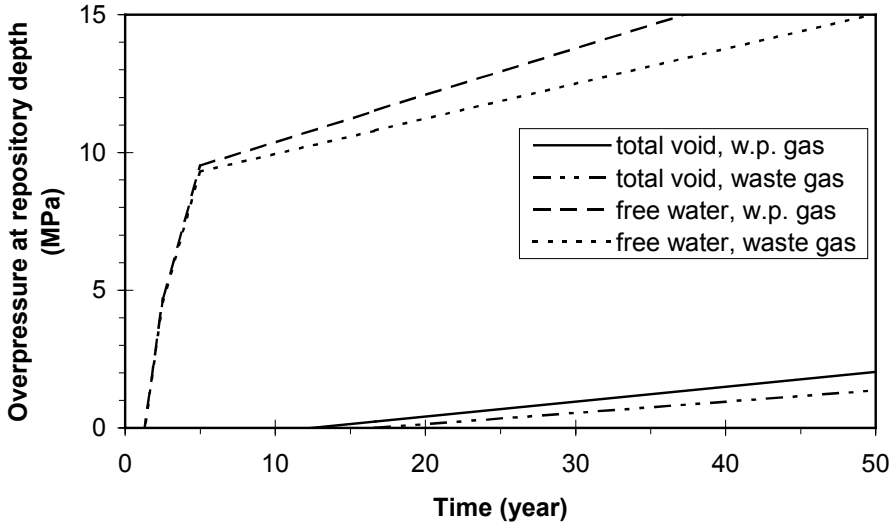

Figure 5-6 Overpressure inside the waste packages in SFL 3 at repository depth as a function of time due to gas generated by the waste (waste gas) and due to gas generated by the waste and packaging material (w.p. gas).

Figures 5-5 and 5-6 together indicate that even if both waste packages and concrete structures initially are intact, the internal gas pressure build-up will probably open up cracks or slits through which gas can escape. This may occur within a short time period of gas generation, a few to some tens of years for the waste packages and less than 200 years for the concrete structures.

5.1.3 Gas escape

Some simple calculations have been carried out to get an indication on the combination of internal overpressure and size of fully penetrating cracks or slits in the concrete structures required for gas to escape at the same rate as it is generated. By assuming that the fractures or slits are planar and of equal size and neglecting the capillary pressure, the gas flow through these fractures or slits could be expressed as (Wiborgh *et al.*, 1986):

$$Q = \frac{A_f \cdot i \cdot k_p}{\mu \cdot L} \Delta P \qquad (5\text{-}1)$$

where:

Q is the gas flow (m^3/s)

A_f is the cross-sectional area of a fracture or slits (m^2)

i is the number of fractures or slits with cross-sectional area A_f

k_p is the permeability of the fracture or slits (m^2)

μ is the dynamic viscosity of the gas (Ns/m^2)

L is the length of the fracture or slit in the flow direction (m)

ΔP is the pressure difference over the structure or wall (Pa)

The permeability of a planar fracture or slit is given by (Wiborgh *et al.*, 1986):

$$k_p = \frac{b^2}{12} \qquad (5\text{-}2)$$

and the cross-sectional area of the fracture or slit could be expressed as:

$$A_f = b \cdot S \qquad (5\text{-}3)$$

where b is the fracture aperture (m), and S is the width of the fracture or slit (m), i.e. the fracture extension perpendicular to the flow direction.

If the fracture or slit contains water, the capillary pressure in the fracture or slit must be exceeded before gas release may occur. The capillary pressure, in a planar fracture or slit is given by:

$$P_c = \frac{2\sigma}{b} \qquad (5\text{-}4)$$

where P_c is the capillary pressure (Pa), and σ is the surface tension (N/m).

These equations have been used to calculate the internal overpressure inside the concrete structures in SFL 3 required for gas escape through fractures in these structures. The calculations were performed for the assumption of fully penetrating fractures in the 0.5 m thick concrete lid, L = 0.5 m. Other input data used were:

$\mu = 8.7 \cdot 10^{-6}$ Ns/m^2

σ = 0.073 N/m

It should be pointed out that the resistance to gas flow in the surrounding bentonite barriers was not considered in these calculations.

The results are depicted in Figure 5-7. The upper diagram shows the capillary pressure versus fracture aperture together with the internal overpressure as a function of fracture aperture for different gas escape rates and assuming that the number of fractures times the fracture width, $i \cdot S$, is equal to 1 m. The selected values of the gas escape rates are equal to the estimated gas generation rates during different time periods (see Figure 5-3).

The lower diagram in Figure 5-7 shows the internal overpressure versus fracture aperture for a gas escape rate equal to the estimated initial gas generation rate of 366 m^3/year and different values of the product of the number of fractures and fracture width. The capillary pressure versus fracture aperture is also displayed in the diagram.

The capillary pressure gives the minimum overpressure required for gas escape. When the capillary pressure is reached, water in the fracture is displaced by gas. Once the fracture is drained gas may escape through the fracture. If the capillary pressure is higher than the pressure required balancing the gas escape rate with the gas generation rate, the gas escape rate will be higher than the gas generation rate thereby lowering the internal overpressure. This continuous until the internal overpressure is decreased down to the value where the gas escape rate balances the gas generation rate. If the capillary pressure is lower than the pressure required for gas escape at the same rate as it is generated, gas escape through the drained fracture will occur at a rate lower than the gas generation rate. This will cause an increase in the internal overpressure and an increase in the gas escape rate which will proceed until the internal overpressure reaches the value of the pressure difference required for gas escape at the same rate as it is generated.

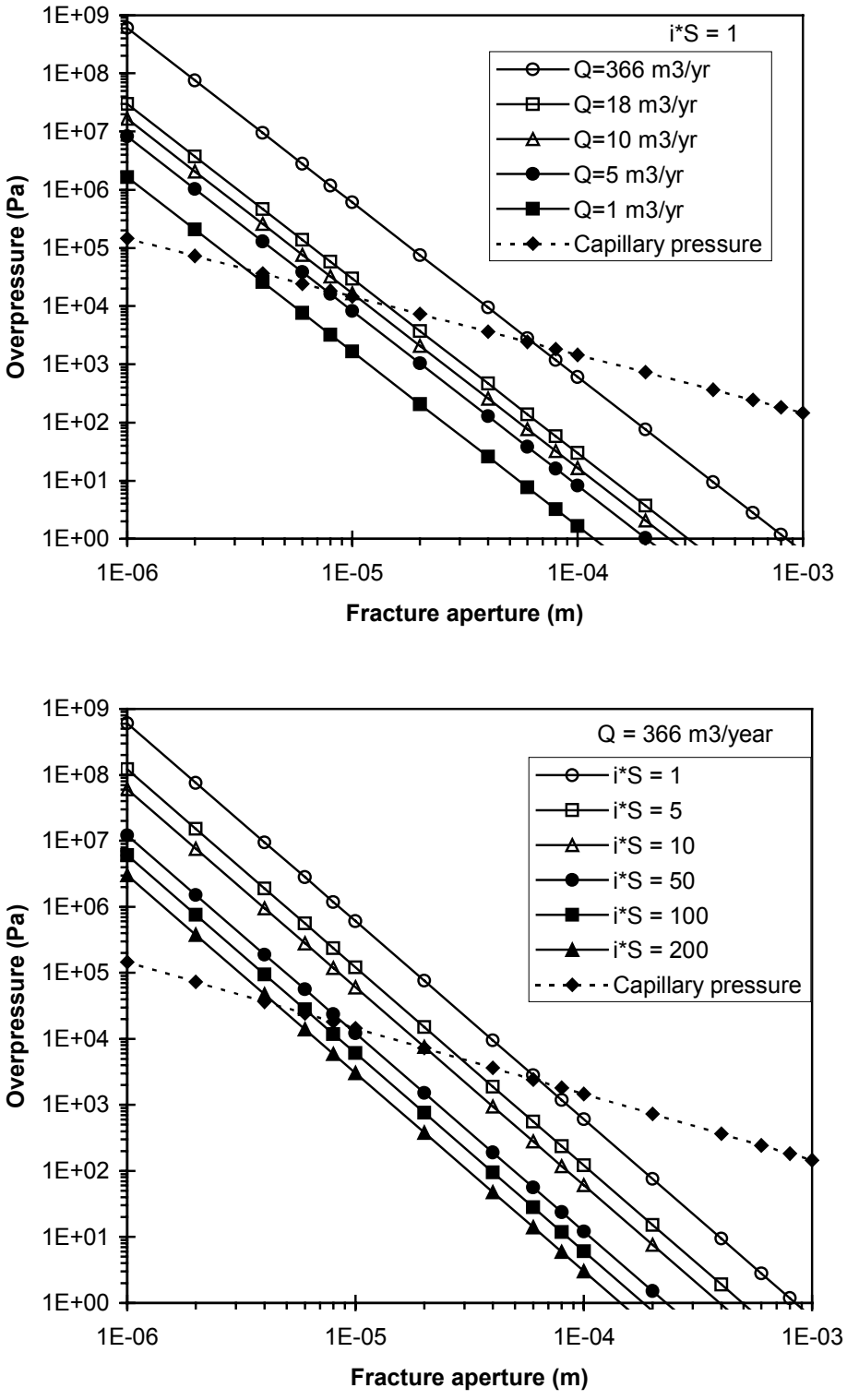

Figure 5-7 Internal overpressure inside the concrete structures in SFL 3 versus fracture aperture for different gas escape rates (upper) and different i·S = number of fractures times fracture width, (lower). The selected gas escape rates represent estimated gas generation rates during different time periods (see Figure 5-3).

The diagrams in Figure 5-7 indicate that the capillary pressure will determine the internal overpressure required for gas escape as long as the fracture apertures are larger than 0.07 mm and the number of fractures times the fracture width is larger than 1 m. Thus, for these combinations of fracture geometry, an internal overpressure of about 2 to 3 kPa is enough to allow gas escape through the concrete lid at the same rate as it is generated, provided that the resistance to gas flow in the surrounding bentonite barrier is negligible. For smaller fracture apertures the required internal overpressure is higher. How much higher depends on the gas escape rate and the number and widths of the fractures. However, the required internal overpressure must always exceed the capillary pressure for the actual fracture aperture. For comparison, the capillary pressure in intact structural concrete is reported to be of the order of 1 – 2 MPa (Moreno and Neretnieks, 1991).

If bentonite barriers surround the concrete structures, the critical overpressure must be reached before gas can escape through these bentonite barriers. In calculations of the gas release from the silo in SFR it was assumed that transport paths for gas in the 90/10 sand-bentonite layer above the lid in the silo are created at an internal overpressure of 50 kPa (Moreno and Neretnieks, 1991). Adopting the same assumptions for the sand/bentonite above the concrete lid in SFL 3 would mean that the internal overpressure required to open up gas channels in the sand/bentonite above the concrete lid is at least 10 times higher than the internal overpressure required for gas flow through fractures in the concrete lid for fracture apertures larger than 0.07 mm if the number of fractures times the fracture width is equal to or larger than 1 m.

Assuming that the capillary pressure, *Pc*, in the largest pores in the sand-bentonite determines the critical pressure and that these pores are circular with a radius *r*, the relation between the capillary pressure and the pore radius is given by:

$$P_c = \frac{2\sigma}{r} \qquad (5\text{-}5)$$

Assuming further that the water in these largest pores is displaced by gas and that gas channels are created in the sand-bentonite once the critical pressure is reached, the steady-state gas flow, *Q*, through these largest pores in the sand-bentonite could be expressed as:

$$Q = \frac{A_{pore} \cdot k_{pore}}{\mu \cdot L_{bent}} \cdot \Delta P \qquad (5\text{-}6)$$

where:

A_{pore} is the cross-sectional area of all pores in the sand-bentonite, through which gas escapes (m^2),

k_{pore} is the pore permeability (m^2),

L_{bent} is the thickness of the sand-bentonite layer (m),

ΔP is the pressure difference over the sand-bentonite layer (Pa).

Equation 5-6 also presumes that the gas transport in the surrounding rock not is a limiting factor.

The permeability of a circular pore with radius *r* is given by:

$$k_{pore} = \frac{r^2}{8} \qquad (5\text{-}7)$$

The relation between capillary pressure and pore radius given in Eq. 5-5 is plotted in Figure 5-8, upper. This diagram shows that a capillary pressure of 50 kPa corresponds to a pore radius of about 3 μm, and that a pore radius of 10 μm would give a capillary pressure of about 10 to 20 kPa.

The lower diagram in Figure 5-8 shows the pressure difference over the1.5 m thick sand-bentonite at a steady-state gas flow of 366 m^3/year through pores with a radius of 3 and 10 μm, respectively, as a function of the total area of the pores accessible to gas flow. This diagram indicates that the steady-state pressure difference required for the estimated maximum gas generation rate will not exceed the capillary pressure as long as the radius of the pores through which gas escapes is larger than 3 μm, and the total cross-sectional area of these pores is larger than 0.003 m^2.

The total cross-sectional area of the sand-bentonite layer above the concrete structure is estimated to be 1 040 m^2, and in case of a 90/10 sand-bentonite, the porosity is 25% (Wiborgh (ed.), 1995). This means that the total cross-sectional area of all pores is about 260 m^2. Thus, the simple calculations described above indicate that only a very small part of the total porosity of the sand-bentonite is required for all gas to escape once the capillary pressure required for displacement of water and developing gas channels in these pores is reached.

Comparing the pressure difference required for gas flow through the sand-bentonite with the pressure difference required for gas flow through the concrete lid indicates that the maximum overpressure inside the concrete structures will be determined by the critical pressure of the sand-bentonite barrier if:

- the concrete lid initially contains fractures or slits, or fractures or slits in the concrete structures are created during the initial period of high gas generation at an internal overpressure below the critical pressure of the sand-bentonite,
- the aperture of the fractures in the concrete lid is larger than 0.07 mm, and the number of fractures times the fracture width is larger than 1, and
- the gas transport capacity in the surrounding rock not is a limiting factor.

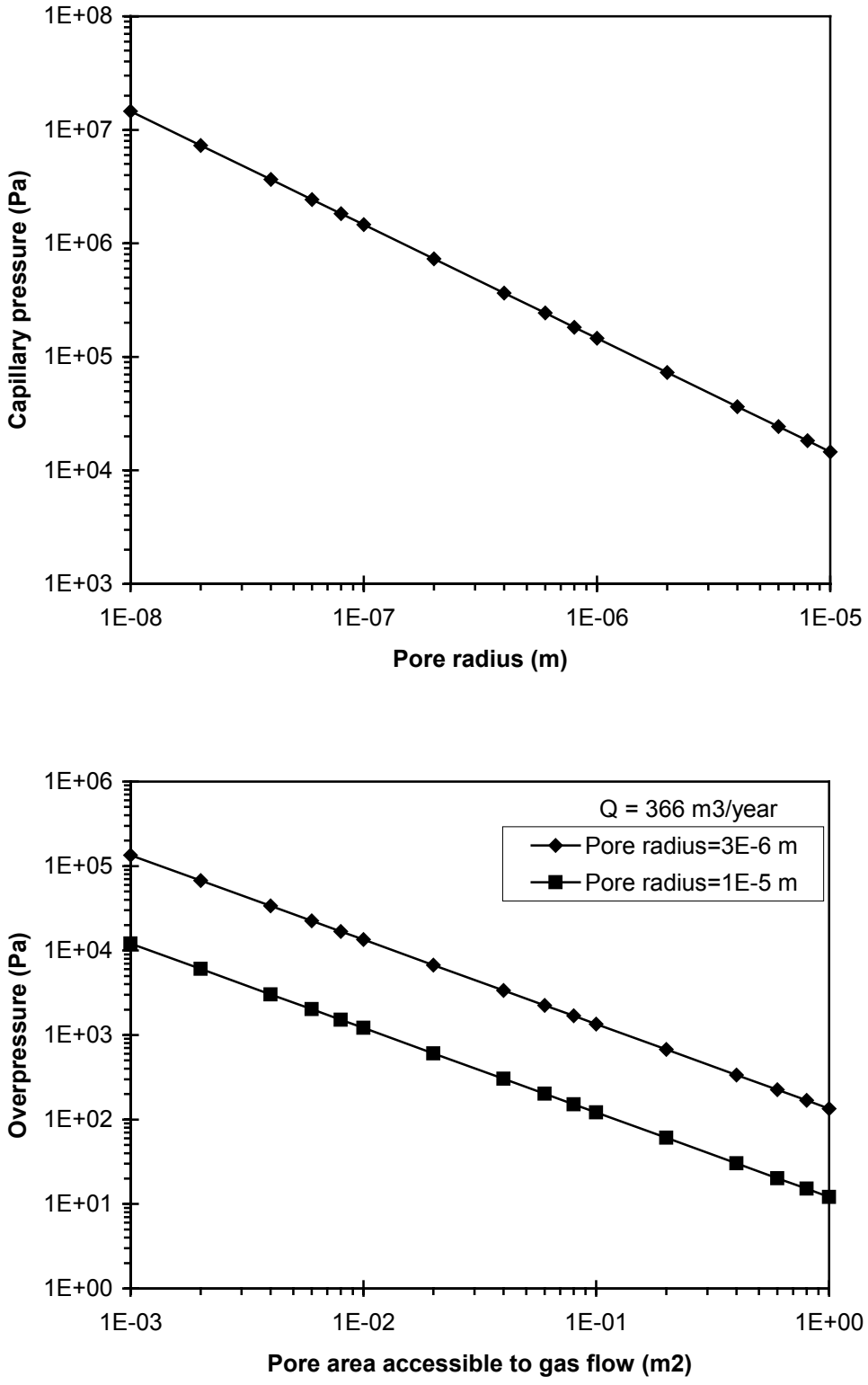

Figure 5-8 Capillary pressure versus pore radius (upper). Steady-state pressure difference over the 1.5 m thick sand-bentonite layer in SFL 3 as a function of the total cross-sectional area of the pores available to gas flow for a gas escape rate equal to the initial gas generation rate in SFL 3 (lower).

Sand/gravel backfill

In the alternative design of SFL 3 the outer barrier is sand/gravel instead of bentonite and sand bentonite. Assuming that the surrounding sand/gravel backfill is water saturated when gas generation is initiated, the capillary pressure in the water-filled pores in the backfill determines the minimum overpressure required for gas escape through the backfill. This capillary pressure is dependent on the pore size distribution in the backfill, which in turn is dependent on the particle size distribution of the backfill material. Experimentally determined capillary pressures in a sand with a mean particle diameter of 0.3 mm and maximum particle diameters in the range 0.4 – 0.5 mm indicates that a capillary pressure of about 2 to 3 kPa is required to decrease the water saturation from 100 % to 90 % (Höst-Madsen, 1989). Data given in Collin and Rasmuson (1986) indicate that a capillary pressure of less than 1 kPa is required to decrease the saturation degree from 100 to 90% in a moraine with the largest particle diameter in the range 0.2 to 2 mm and a permeability of 10^{-13} m^2, and less than 0.1 kPa in a sand with a permeability of 10^{-11} m^2.

Neglecting the gas transport inside the concrete structure as well as in the surrounding rock, Eq. 5-6 can be used to calculate the internal overpressure required for steady-state gas escape through the surrounding 1.5 m thick sand/gravel backfill. For a gas flow equal to the initial gas generation rate of 366 m^3/year and assuming gas escape through the backfill placed on top of the waste (A = 1 040 m^2) where 1% of the porosity of the backfill ($\varepsilon = 0.3$) is available to gas flow, the following relation between the pore permeability, k_p, and pressure difference, ΔP, is obtained:

$$\Delta P = \frac{4.9 \cdot 10^{-11}}{k_{pore}} \qquad [N/m^2 = Pa] \qquad (5\text{-}8)$$

Thus, for a pore permeability of $4.9 \cdot 10^{-11}$ m^2 or larger, the required internal overpressure will be 1 Pa or less. Assuming that the pores in the backfill through which gas escapes are circular with a uniform radius, a pore permeability of $4.9 \cdot 10^{-11}$ m^2 corresponds to a pore radius of 20 μm. If the radius of the largest pores in the backfill are larger than this, the pore permeability will be larger and the pressure difference during gas escape lower than 1 Pa.

After cracking of the waste packages and concrete structures these simple calculations together with the experimental data cited above suggests that gas escape from SFL 3 with sand/gravel as outer barrier probably will occur without major internal pressure build-up. The maximum internal overpressure will most likely be determined by the pressure required to displace water in the largest pores in the sand/gravel backfill thereby open up gas channels in the backfill. This capillary pressure is dependent on the particle size distribution of the backfill, but as long as more clay type materials are avoided, the internal overpressure will probably not be higher than 0.1 to 1 kPa.

5.2 SFL 4

5.2.1 Gas generation rates and volumes

The only gas generating process in SFL 4 is corrosion of steel in waste and packagings, since no reinforced concrete structures or organic materials will be present in this part of

the repository. The estimated gas generation rate as a function of time is shown in Figure 5-9, and the initial gas generation rate and the maximum theoretical gas volume that can be generated at repository depth is given in Table 5-3. The initial gas formation rate is estimated to be about 24 m^3/year at repository depth. The waste in the cubic steel vessels contributes with almost 20 m^3/year and the cubic steel vessels with almost 4 m^3/year. The duration of the corrosion and gas generation is estimated to be 3 000 years for the steel vessels and 2 250 – 6 500 years for the waste in the steel vessels. The gas generation rate from corrosion of the transport casks and containers is small, less than 0.5 m^3/year, but it will take 150 000 years of corrosion before the most thick-walled transport casks are corroded away.

The gas volume at repository depth generated by corrosion is shown in Figure 5-10 as a function of time. After 6 500 years when the steel in the waste and in the packaging is corroded away, almost 80 000 m^3 of gas has been generated. Corrosion of the transport casks and containers will continue to generate gas. After 150 000 years the total volume of gas generated is almost 110 000 m^3 at repository depth (see also Table 5-3).

Table 5-3 Initial gas generation rates and maximum theoretical gas volume at 500 m depth generated by corrosion of steel in SFL 4.

	Initial gas generation rate, [m^3/year]	Maximum theoretical gas volume, [m^3]
Waste	19.6	62 640
Packaging	3.7	11 060
Transport casks and containers	0.4	34 000
Total	**23.7**	**107 700**

The amount of water required maintaining hydrogen-evolving corrosion during the first 2 250 years is estimated to be about 2 130 m^3 (Appendix C). This water volume corresponds to approximately 25% of the water contained in the waste packages and in the transport casks and containers at full saturation. The maximum theoretical volume of gas that can be generated by corrosion of metals in SFL 4 would require a water volume of about 4 310 m^3. This is slightly more than half of the water volume in the waste packages, transport casks and transport containers at full saturation.

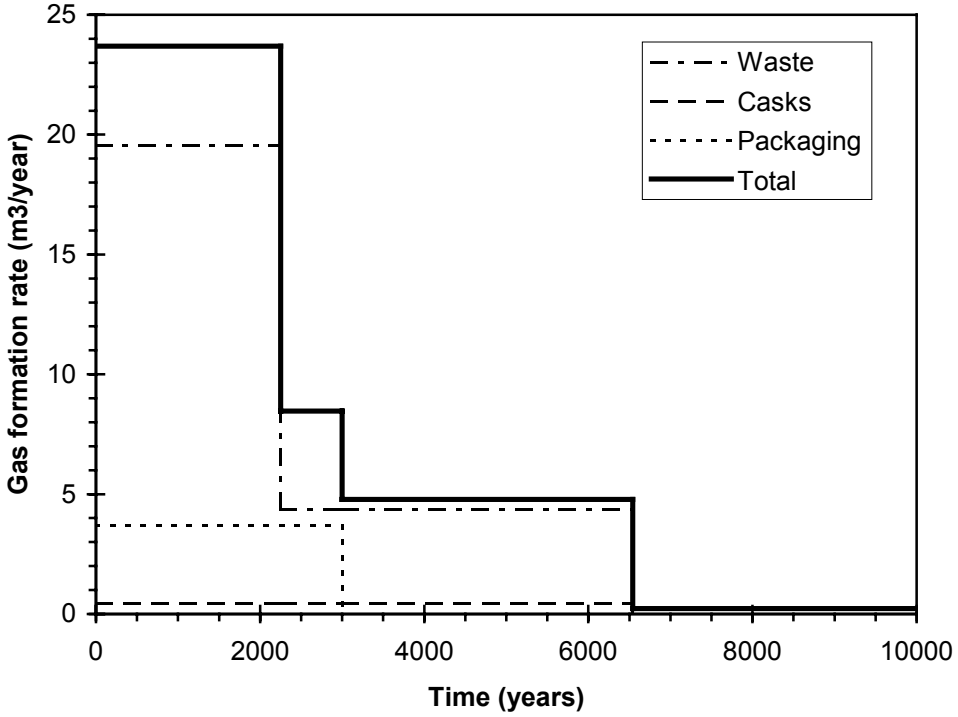

Figure 5-9 Gas formation rates at repository depth due to corrosion of steel in SFL 4.

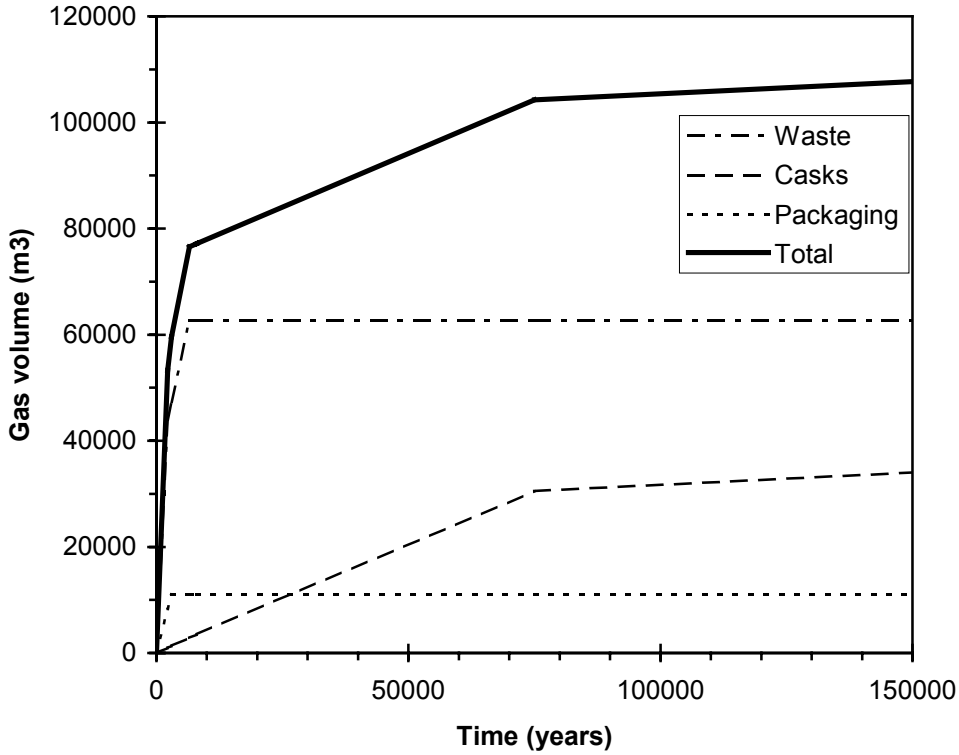

Figure 5-10 Volumes of hydrogen gas generated at repository depth by steel corrosion in SFL 4.

5.2.2 Pressure build-up and gas escape

The only engineered barrier surrounding the waste packages, transport casks and transport containers in SFL 4 is the backfilled sand or gravel in the tunnel. If the gas generated cannot escape through the waste packages and the transport casks and containers and through the surrounding backfill at the same rate as it is generated, the internal pressure will start to increase when the internal void accessible to gas is exceeded.

During the first 2 250 years of corrosion approximately 53 300 m^3 of gas (at repository depth) is generated. This gas volume is more than 6 times the void in the waste packages, transport casks and transport containers, and about 4.5 times the total void in the tunnel. The time required to generate a gas volume equal to the internal void in the different waste packages and transport casks varies between about 200 and 5 600 years (see Tables 6 and 7 in Appendix B). This means that sometime during the first 5 600 years of corrosion, an overpressure will be created inside the waste packages, transport casks and transport containers.

In order to achieve the gas generation rates shown in Figure 5-10 water must be able to penetrate the steel vessels, transport casks and transport containers during saturation of the repository or later. If the waste packages, transport casks and transport containers not are water tight, they probably not are gas tight either. Therefore it seems reasonable to neglect the gas transport resistance in the waste packages, transport casks and transport containers.

If the surrounding sand/gravel backfill is water saturated when gas generation is initiated, the capillary pressure in the water-filled pores in the backfill determines the minimum overpressure required for gas escape through the backfill. This capillary pressure is dependent on the pore size distribution in the backfill, which in turn is dependent on the particle size distribution of the backfill material

Neglecting the gas transport resistance in the waste packages, the transport casks and transport containers as well as in the surrounding rock, Eq. 5-6 can be used to calculate the internal overpressure required for steady-state gas escape through the surrounding 1 m thick sand/gravel backfill. For a gas flow equal to the initial gas generation rate of 23.7 m^3/year and assuming gas escape through the backfill placed on top of the waste (A = 3 200 m^2) where 1% of the porosity of the backfill ($\varepsilon = 0.3$) is available to gas flow, the following relation between the pore permeability, k_p, and pressure difference, ΔP, is obtained from Eq. 5-6:

$$\Delta P = \frac{6.8 \cdot 10^{-13}}{k_{pore}} \qquad [N/m^2 = Pa] \qquad (5\text{-}9)$$

Thus, for a pore permeability of $6.8 \cdot 10^{-13}$ m^2 or larger, the required internal overpressure will be 1 Pa or less. Assuming that the pores in the backfill through which gas escapes are circular with a uniform radius, a pore permeability of $6.8 \cdot 10^{-13}$ m^2 corresponds to a pore radius of 2.3 μm. If the radius of the largest pores in the backfill are larger than this, the pore permeability will be larger and the pressure difference during gas escape lower than 1 Pa.

These simple calculations together with the experimental data cited in section 5.1.3 suggests that gas escape from the waste contained in SFL 4 probably will occur without major internal pressure build-up. The maximum internal overpressure will most likely be determined by the pressure required to displace water in the largest pores in the

sand/gravel backfill thereby open up gas channels in the backfill. This capillary pressure is dependent on the particle size distribution in the backfill, but as long as more clay type materials are avoided, the internal overpressure will probably not be higher than 0.1 to 1 kPa.

5.3 SFL 5

5.3.1 Gas generation rates and volumes

In SFL 5 gas will be generated by corrosion of metals in the waste packages and by corrosion of steel reinforcements in the concrete structures. The estimated gas generation rate as a function of time is shown in Figure 5-11. The initial gas generation rate and the maximum theoretical gas volume that can be generated at repository depth is given in Table 5-4. The initial gas generation rate is estimated to be almost 8 m^3/year at repository depth. The waste and the steel cassette inside the waste packages each contribute with almost 3 m^3/year. After 3 000 years of corrosion, the steel cassettes are corroded away and the total gas generation rate will decrease to about 3.7 m^3/year. Corrosion of the steel in the waste will proceed for about 100 000 years before the most thick-walled components are corroded away. Because of the slow corrosion of Zircalloy, the waste will continue to generate gas during an additional 20 000 years, but at a rate below 0.01 m^3/year. The reinforcement bars in the packaging as well as in the concrete structures will initially generate gas at a rate of about 1 m^3/year, and the corrosion will proceed for approximately 8 000 years.

Table 5-4 Initial gas generation rates and maximum theoretical gas volume at 500 m depth generated by corrosion of metals in SFL 5.

	Initial gas generation rate, [m^3/year]	Maximum theoretical gas volume, [m^3]
Waste	3.0	20 210
Steel	3.0	19 920
Zircalloy	$2 \cdot 10^{-3}$	290
Packaging	4.0	13 590
Steel cassettes	2.9	8 830
Reinforcement bars	1.1	4 760
Concrete structures	0.9	3 660
Total	**7.9**	**37 460**

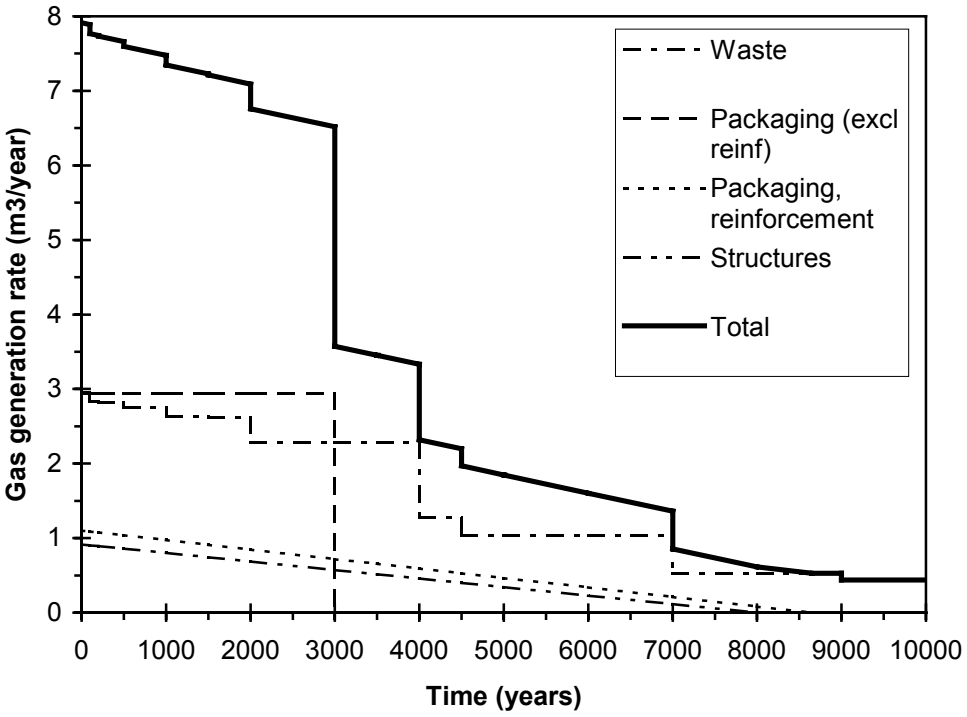

Figure 5-11 Gas generation rates at repository depth due to corrosion of steel and Zircalloy in SFL 5.

The gas volume generated at repository depth by corrosion in SFL 5 as a function of time is depicted in Figure 5-12. After 3 000 years when the steel cassettes in the waste packages are consumed approximately 23 000 m^3 of gas has been generated. After 20 000 years of corrosion, most of the steel in the waste will be corroded away and the total generated gas volume is approximately 35 000 m^3. During the next 100 000 years, only about 2 000 m^3 of gas will be generated, leading to a total gas volume after 120 000 years of about 37 500 m^3 at repository depth (see also Table 5-4).

The maximum volume of gas that theoretically may be formed, and the estimated volumes of gas formed by corrosion after 1 year and 3 000 years are given for the different waste categories (waste and packaging) in Tables 8 – 10 in Appendix B. The largest amounts of gas is generated by the waste packages with control rods ('Contr. Rods'), and with moderator tank covers ('Tank cover') from BWR reactors. Large amounts are also generated by the BWR waste category 'Tank', and by the PWR waste categories 'Tank' and 'Internal parts'. The time of gas generation required to form a gas volume equal to the total void in the waste packages is of the order of 200 to 600 years.

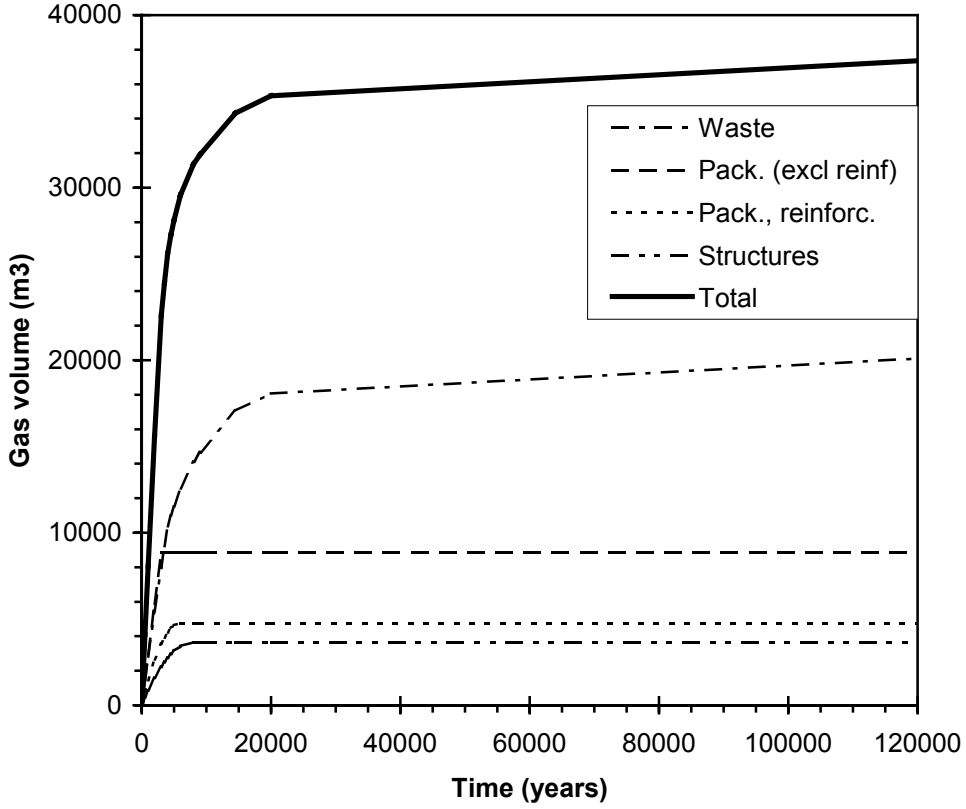

Figure 5-12 Volumes of hydrogen gas generated at repository depth by corrosion of steel and Zircalloy in SFL 5.

About 815 m^3 of water is required to maintain hydrogen-evolving corrosion of all steel and Zircalloy in the waste packages in SFL 5 during 3 000 years (Appendix C). This volume corresponds to about 30% of the water in the waste packages at full saturation, and to about 13% of the water in the waste packages and in the concrete compartments at full saturation. Approximately 1 350 m^3 of water is required to corrode away the total amount of metals in the waste packages, i.e. about 50% of the water in the waste packages and about 20% of the total amount of water inside the concrete compartments at full saturation. Consumption of all the reinforcement bars in the concrete structures by hydrogen evolving corrosion requires about 150 m^3 of water, i.e. about 30% of the water contained in the structures at full saturation.

5.3.2 Pressure build-up

The increase in gas pressure in the waste packages and inside the concrete compartments as a result of gas generation and accumulation has been estimated. The results are shown in Figures 5-13 and 5-14 as overpressure at repository depth versus time assuming either that the estimated total void are accessible to gas, or that the volume accessible to gas is equal to the volume of free water. Using the same assumptions as were used to calculate the amount of free water in SFL 3 (see 5.1.2), the free water volume in the waste packages is about 15 000 m^3 and the total free water volume inside the concrete structures is about 4 900 m^3. The void between the waste packages contributes with 3 400 m^3 to the total free volume.

Figure 5-13 indicates that if gas cannot escape from the waste packages, an overpressure inside the packages will be created after a few hundreds of years up to at most 500 years. If gas accumulation proceeds, the internal overpressure will increase to a level of at least about 4 – 5 MPa after 1 000 years of corrosion. The capillary force in intact structural concrete is of the order of 1 to 2 MPa. This means that gas will displace water in the pores in the concrete container and escape from the containers once this pressure level is reached even if the waste packages initially are gas tight. However, the gas pressure itself or the water that is pressed out through the container walls as gas generation proceeds, will probably create high enough forces to cause cracks in the concrete containers or open up slits in the waste packages, e.g. between the lid and walls of the containers, at a significantly lower internal overpressure than 1 MPa. It seems therefore reasonable to assume that gas escape from the waste packages will be initiated sometime during the first 500 years of corrosion.

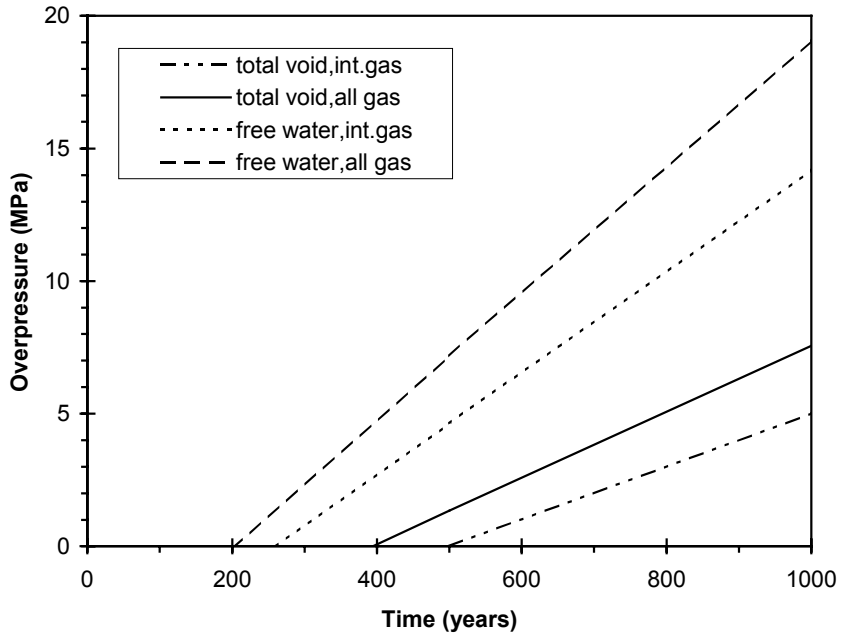

Figure 5-13 Overpressure inside the waste packages in SFL 5 at repository depth as a function of time due to accumulation of gas generated by corrosion of the inner steel cassette and metals in the waste (int.gas), and by all metals in the waste packages (all gas).

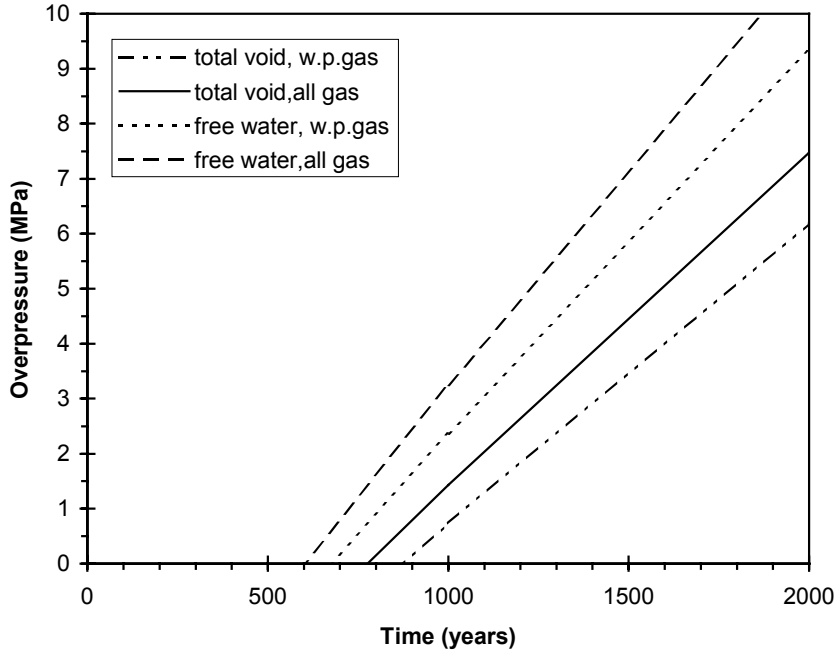

Figure 5-14 Overpressure inside the concrete structures in SFL 5 at repository depth as a function of time due to accumulation of gas generated by the waste packages and by corrosion of reinforcements in the structures (all gas), and by gas generated by the waste packages only (w.p.gas).

Figure 5-14 shows that accumulation of gas generated by corrosion of metals in waste and packaging (w.p.gas) in the total void inside the concrete structures will lead to a pressure build-up of 0.5 to 1 MPa after 1 000 years. Including also gas generated by corrosion of reinforcements in the concrete structures (all gas) the overpressure after 1 000 years is estimated to be about 1.5 MPa. If the void accessible to gas is equal to the estimated free water volume inside the concrete structures it will take 700 to 800 years of gas generation and accumulation to reach an internal overpressure of 1 MPa. Again considering that the silo in SFR is constructed for a maximum internal overpressure of 280 kPa (Moreno and Neretnieks, 1991) it seems reasonable to assume that even if the concrete structures are intact initially, the internal pressure build-up will create cracks or fractures in the structures at a lower internal overpressure than 1 MPa. Thus, according to Figure 5-14, gas escape through the concrete structures will be initiated in less than 1 000 years of corrosion.

5.3.3 Gas escape

The internal overpressure required for gas escape through fractures in the concrete structures in the SFL 5 vaults is estimated by applying Eqs 5-1 to 5-4. The calculations are carried out assuming fully penetrating fractures in the 0.3 m thick concrete lid, and neglecting any resistance to gas flow in the sand/gravel backfill surrounding the concrete structures.

The results are shown in Figure 5-15 as the pressure difference over the concrete lid versus the fracture aperture for a gas escape rate equal to the estimated initial gas generation rate

of 7.9 m^3/year and different values of the product of the number of fractures and fracture width. In addition, the capillary pressure as a function of fracture aperture is depicted in the figure. It should be pointed out that this initial gas generation rate is the total rate for all three vaults, and consequently, the assumed values of number of fractures times the fracture width are also for all three vaults. This means that the product $i \cdot S = 3$ m could, for example, represent a case where each vault contains one fracture which is 1 m wide.

Figure 5-15 indicates that the capillary pressure will determine the internal overpressure required for gas escape at the same rate as it is generated for fracture apertures of about 10 μm and larger provided that the number of fractures times the fracture width is not smaller than 1 m. Thus, for a fracture aperture of about 10 μm and the product of number of fractures and fracture width equal to 1 m or larger, an internal overpressure of about 20 kPa would be enough to allow gas escape at the same rate as it is generated. For smaller fracture apertures a higher internal overpressure is required. How much higher depends on the fracture width and number of fractures, but the overpressure must always exceed the capillary pressure for the actual fracture aperture.

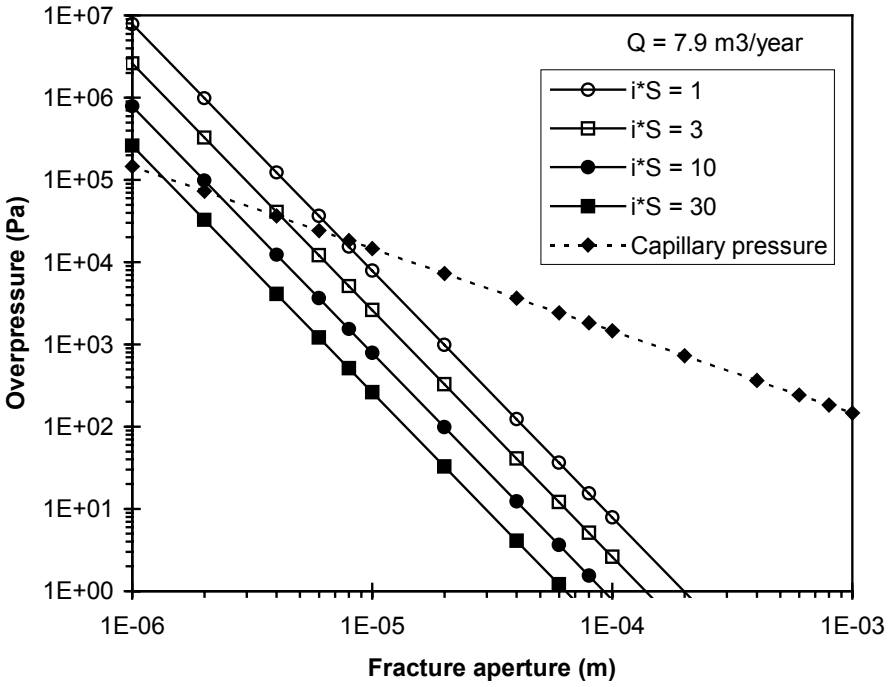

Figure 5-15 Internal overpressure inside the concrete structures in SFL 5 versus fracture aperture for a gas escape rate equal to the initial gas generation rate and different values of the number of fractures times the fracture width (i·S).

The concrete structures in the SFL 5 vaults will be surrounded by sand/gravel backfill of similar type as in SFL 4. The initial gas generation rate in SFL 5 is about 3 times lower than in SFL 4 and the geometry of the backfill on top of the waste is similar. Thus, the simple calculations made of the gas transport capacity in the sand/gravel backfill in SFL 4 and the data on capillary pressures cited in section 5.2.2 indicate that the pressure difference required for creating gas channels in the backfill in SFL 5 and for gas to escape through these channels probably not will be higher than 0.1 to 1 kPa.

6 Effects on radionuclide release from SFL 3

6.1 General

Metal corrosion and gas generation may mechanically affect the waste packages and concrete structures in SFL 3-5 by formation of volume expanding corrosion products and by creating high internal gas pressures. If this leads to fracturing or cracking of the engineered barriers, the transport paths and transport rates of escaping radionuclides will be affected. In addition, gas generation and a build-up of internal gas pressures will expel water from the interior of the repository vaults, and may also affect the hydraulic situation in the repository in a longer time perspective. This may also have implications on the release of radionuclides from the repository.

Calculated gas generation rates and pressure build-up given in Chapter 5, calculated volume increase caused by iron corrosion products given in Appendix D and calculated amount of water that can be displaced given in Appendix E gives a background to the radionuclide release calculations.

The consequences of gas generation in SFL 3-5 depends on the gas generation rates and volumes, but also on the states of the different barriers when gas generation starts. After repository closure, intruding groundwater will gradually saturate the repository barriers and waste packages. Because the repository is proposed to be located at 500 m depth, the repository barriers and waste packages may be exposed to a hydraulic gradient as large as 5 MPa during the saturation phase. If so, it is possible that cracks are formed in concrete structures and concrete packagings and that steel packagings, if they initially are tight, are damaged to allow water to enter. To include this potential effect of the hydrostatic pressure during the saturation phase, different assumptions concerning the states of the barriers at the initiation of gas generation has are made when estimating the effects of gas generation.

Another aspect of the saturation phase that may affect both gas generation rates and the consequences of gas generation is the duration of the saturation phase. A slow inflow of water may initiate gas-generating processes at different times in different parts of the repository. This could have large effects on the gas generation rate in SFL 3 because it contains aluminium that have a high corrosion and rate and therefore are corroded away relatively fast. A distribution of the starting times for corrosion of aluminium in different parts of SFL 3 would therefore decrease the gas generation rate during the initial phase. However, it would also prolong the initial phase during which corrosion of aluminium may lead to higher gas generation rates than caused by corrosion of steel only. The duration of the saturation phase is not considered here. Instead it is assumed that the entire repository is filled with water when the gas generating processes start, and that these processes are initiated at the same time in the entire repository.

Volume expansion of corrosion products probably gives negligible effect, possibly cracking around reinforcement causing weaknesses but no fully penetrating fractures or cracks.

In case of intact concrete structures surrounded by bentonite barriers in SFL 3, the internal gas pressure will have to increase until fractures or cracks are created in the

structures and the capillary pressure in these fractures and in the surrounding bentonite barriers are exceeded before gas can escape.

Some simple calculations have been made in order to illustrate the effect of gas generation on radionuclide release from SFL 3. These calculations are made assuming either bentonite barriers or sand/gravel backfill outside the concrete structures in SFL 3. It should be noted that the calculations are performed for the old design of SFL 3 and with the earlier waste inventory, i.e. with the same presumptions as in the prestudy of SFL 3-5 (Wiborgh (ed.), 1995). The models and input data used are also the same as those used for the radionuclide migration calculations in the prestudy. The calculation cases comprise one case where bentonite and sand/bentonite is used as backfill and two cases where sand/gravel is used as backfill. In the case with bentonite barriers and in one of the cases with sand/gravel backfill the consequence of an internal build-up of gas pressure is considered. In the other case with sand/gravel as backfill it is assumed that gas can escape without creating high internal gas pressure. This latter case is the same as the case analysed in the prestudy of SFL 3-5, but with a sand/gravel backfill instead of bentonite barriers in SFL 3. The calculation cases and the results of the calculations are described in the following sections of this chapter.

6.2 Cases, assumptions and input data

The release rate of some radionuclides from the engineered barriers in SFL 3 have been calculated for the following three cases:

A. The concrete structure in SFL 3 is surrounded by sand/gravel backfill. Gas that is generated inside the structures can escape through small fractures and/or slits in the waste packages and concrete structures. Radionuclides dissolved in the water inside the waste packages are transported by diffusion inside the concrete structure. Once released from the concrete structures the transport through the sand/gravel backfill occurs by both diffusion and the water flowing in the sand/gravel backfill.

B. The concrete structure in SFL 3 is surrounded by sand/gravel backfill. The concrete structure is intact except for one fracture in the concrete bottom. Gas generated inside the concrete structure cannot escape and the internal gas pressure increases. This results in a displacement of ‘free’ water in the interior of the concrete structure through the fracture in the bottom. The whole interior of the concrete structure is emptied of its free water before gas can escape and the internal gas pressure is decreased. Radionuclides are dissolved in the water in the waste packages. This water with its content of radionuclides is expelled through the fracture in the concrete bottom out into the sand/gravel backfill. When the concrete structure is emptied of free water, radionuclides are transported by diffusion in the concrete structures and by both diffusion and advection in the sand/gravel backfill.

C. The concrete structure in SFL 3 is surrounded by bentonite barriers, pure self-compacted bentonite outside the walls and 90/10 sand/bentonite above the lid and 85/15 sand/bentonite beneath the bottom of the concrete structure. The lid of the concrete structure contains small fractures/openings through which gas can escape, but an internal overpressure of about 50kPa has to be reached before gas can escape through the sand/bentonite above the lid. The pressure increase will displace water from the interior of the concrete structure. It is assumed that the water is displaced

through a fracture in the bottom of the concrete structure, but also into the walls and lid of the concrete structure since the sand/bentonite beneath the bottom will constitute a resistance for flow through the fracture. Radionuclides are dissolved in the water in the waste packages. The quantity of contaminated water displaced corresponds to the volume of free water in the waste packages in the upper 5 metres of the concrete structure. When an internal overpressure of 50 kPa is reached, no more water is displaced and the subsequent transport of radionuclides occurs by diffusion through the concrete structures and bentonite barriers.

In the prestudy of SFL 3-5 (Wiborgh (ed.), 1995), the release of radionuclides was calculated for a reference case. In this reference case the concrete structure in SFL 3 is surrounded by bentonite barriers, but any affects of gas generation inside the structures on the release of radionuclides were neglected. In this case it is assumed that the release of radionuclides takes place via diffusion through the concrete and bentonite barriers in SFL 3. This reference case is described in Lindgren and Pers (1994) and summarised in Appendix G of this report.

The radionuclides studied are organic ^{14}C, ^{59}Ni, ^{129}I and ^{135}Cs. Organic ^{14}C was not included in the reference case calculations within the prestudy. Therefore the release of ^{14}C in case of bentonite barriers is calculated as a part of this study. For all cases studied it is assumed that 10% of the content of ^{14}C in the waste is organic and that organic ^{14}C does not sorb in any of the barriers.

6.2.1 Case A: Sand/gravel backfill and no effects of gas

This case corresponds to the reference case in the prestudy (Lindgren and Pers, 1994/Appendix G). The difference is that the concrete structure is surrounded by a sand/gravel instead of bentonite and sand/bentonite barriers. The hydraulic conductivity in sand/gravel is higher than in sand/bentonite and bentonite. This means that transport by advection becomes important and the size of the water flow in the sand/gravel must therefore be determined.

Water flow

In the prestudy of SFL 3-5, the water flow in the sand/gravel backfill in SFL 4 and SFL 5 was calculated with an analytical model (Lindgren and Pers, 1994). The same model is used here to calculate the water flow in the sand/gravel backfill in SFL 3. The model is further described in Appendix F. The vault dimensions used as input to the calculations are a length of 82 m and a cross sectional area of 250 m^2, corresponding to a diameter of 18 m. Two combinations of hydraulic conductivity and hydraulic gradient in the surrounding rock were applied, a hydraulic conductivity of 10^{-9} m/s together with a gradient of 0.003 and a hydraulic conductivity of 10^{-8} m/s together with a gradient of 0.0003. Both combinations result in a water flux in the surrounding rock of 0.1 litre/m^2, year.

The water flow in the vault was calculated as a function of the average hydraulic conductivity in the vault, see Figures 6-1 and 6-2. The maximum flow, 0.41 m^3/year, is obtained for a groundwater flow in the rock that is parallel to the length of the vault. The figures show that this maximum flow is obtained if the average hydraulic conductivity in the vault is larger than about 10^{-5} to 10^{-6} m/s. This maximum value of the water flow

is chosen for the calculations of radionuclide release in the cases where sand/gravel is used as backfill in SFL 3.

The water flow inside the vault will be distributed between the concrete structure and sand/gravel in proportion to their flow resistance. The hydraulic conductivity in the backfill is of the order of 10^5 times higher than in the concrete structure (see Table 3 in Appendix G). This means that only a very small part of the flow will pass through the concrete structure and this flow is therefore neglected.

The water flow through the sand/gravel at the top, sides and bottom is distributed in proportion to their cross sectional area, assuming flow from the concrete construction to the surrounding rock.

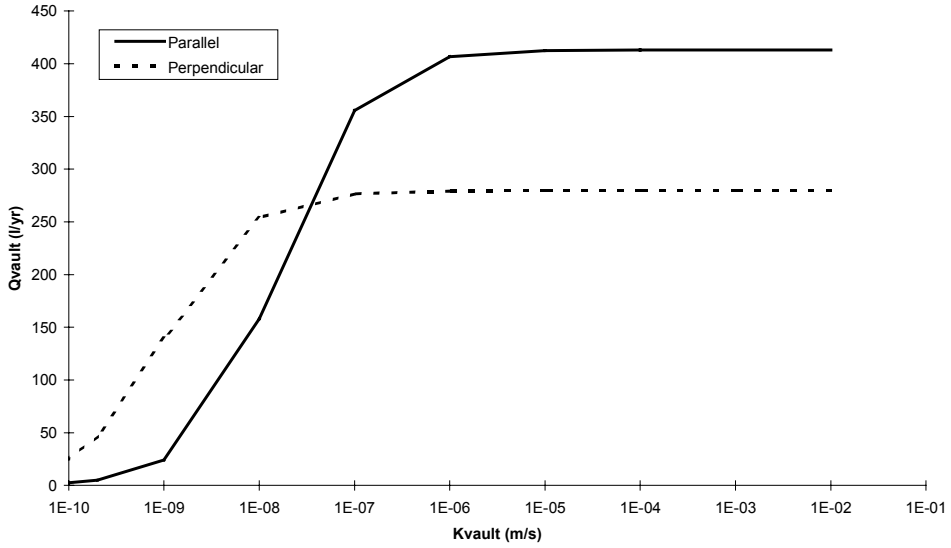

Figure 6-1 Water flow (litres/year) in the SFL 3 vault as a function of the average hydraulic conductivity in the vault. (The hydraulic conductivity in the rock is 10^{-9} m/s and the hydraulic gradient is 0.003.)

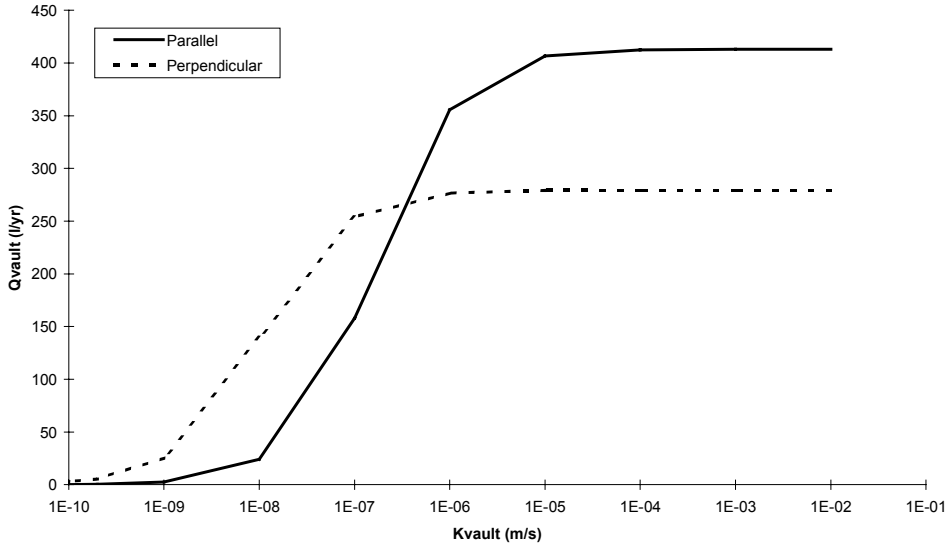

Figure 6-2 Water flow (litres/year) in the SFL 3 vault as a function of the average hydraulic conductivity in the vault. (The hydraulic conductivity in the rock is 10^{-8} m/s and the hydraulic gradient is 0.0003.)

Release calculations

A schematic illustration of how the radionuclide release is conceptualised in the calculations is shown in Figure 6-3. Radionuclides dissolved in the water in the waste packages are released from the packages and transported by diffusion through the surrounding porous concrete into the internal walls of the structure and out through the external walls, lid and bottom of the concrete structure. Radionuclides released from the concrete structure are transported through the sand/gravel by diffusion and by the water flow in the backfill.

Material data and initial conditions used in the calculations are the same as those reported for the reference case with bentonite barriers in Lindgren and Pers (1994) and in Appendix G. The mesh dimensions in the numerical model used are also the same as in Lindgren and Pers (1994) see Appendix G, but the bentonite and sand/bentonite is replaced by sand/gravel, see Figure 6-4. The boundary conditions at the outside border of the sand/gravel barriers are a free flow boundary, i.e. flow into an infinite medium.

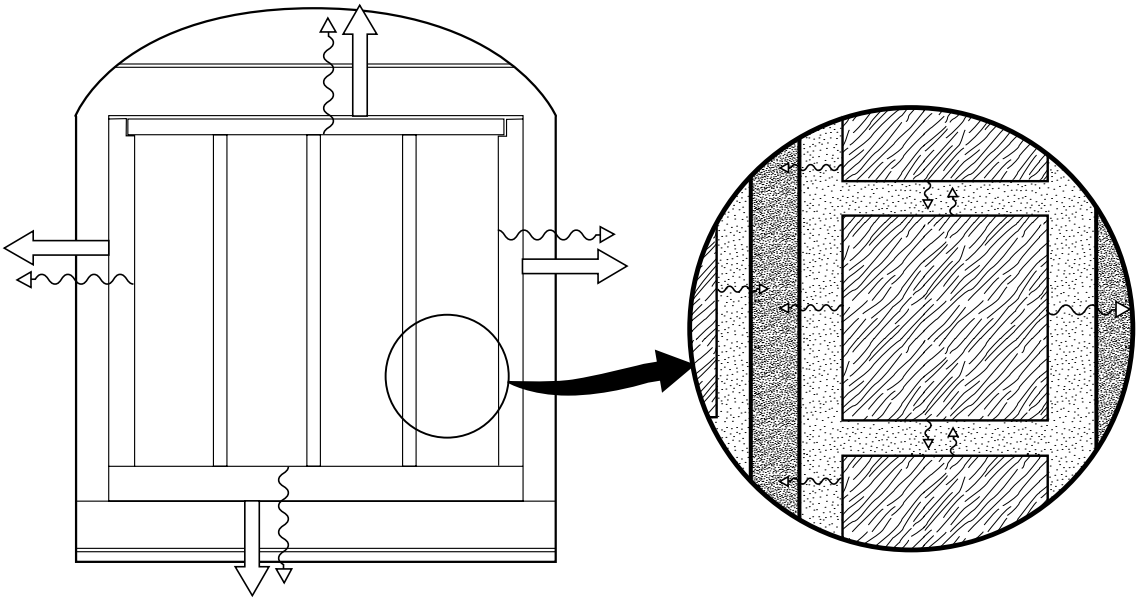

Figure 6-3 Schematic illustration of the release path in the base case.

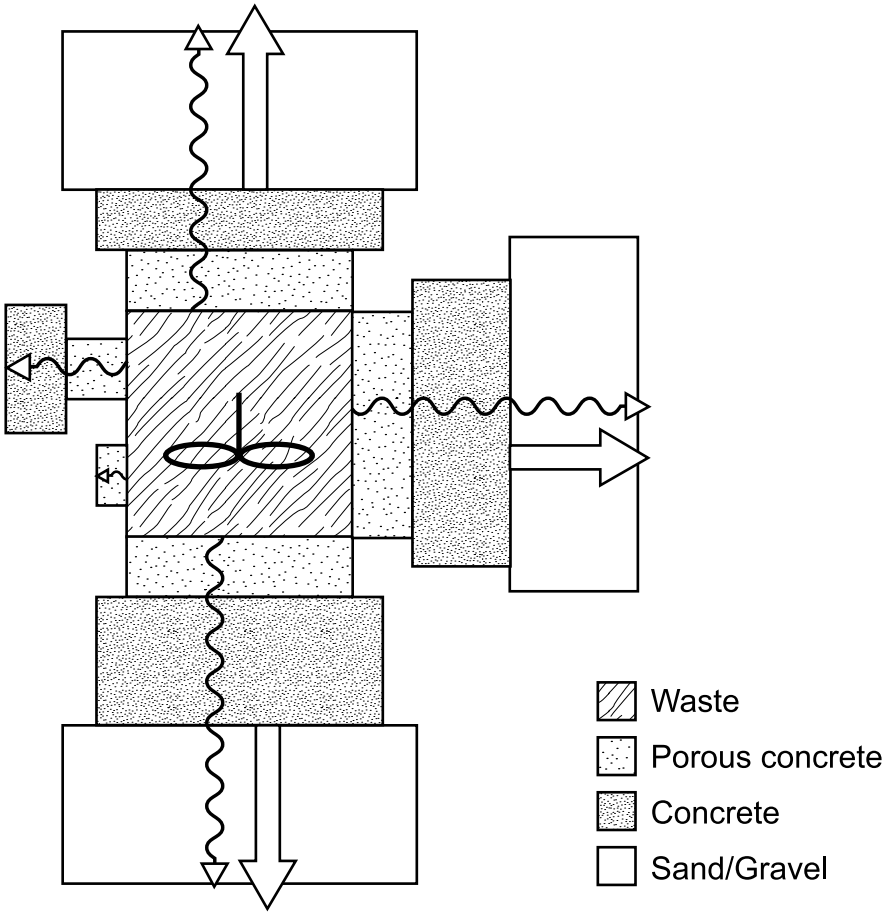

Figure 6-4 Schematic illustration of the mesh geometry in SFL 3 with sand/gravel as outer barrier.

6.2.2 Case B: Sand/gravel backfill and displacement of water by gas

In the calculations, the release of radionuclides is divided into two phases. In the first phase, the displacement of water by gas will cause a plug flow of water through the fracture in the bottom of the concrete structure. During this time, the total amount of free water in the waste packages, as well as its content of radionuclides, is displaced. Since the resistance to flow is considerable higher in the concrete structures than in the fracture and the sand/gravel backfill it is assumed that the whole volume of water is displaced through the fracture out to the sand/gravel beneath the bottom of the concrete structure. This volume of water is estimated to be 474 m^3 (see Appendix E). It is further assumed that the porous concrete surrounding the packages does not constitute any resistance to flow and the potential sorption capacity in the porous concrete is neglected.

In the second phase, gas is no longer affecting the release. The radionuclides still remaining in the waste packages are released by diffusion through the porous concrete and concrete structures out to the surrounding sand/gravel. These radionuclides as well as the radionuclides pushed out to the sand/gravel during the first phase are then transported by diffusion and advection in the sand/gravel to the surrounding rock.

Plug flow phase

It is assumed that gas will cause a plug flow of contaminated water through the fracture in the bottom of the concrete structure. Accounting for sorption in the sand/gravel, the penetration depth into the sand/gravel beneath the bottom of the structure is calculated as follows:

$$depth = \frac{V_0}{A(\varepsilon + K_d \rho_s (1-\varepsilon))} \qquad (6\text{-}1)$$

where

V_0 = volume of contaminated water (m^3)

A = cross sectional area of the sand/gravel beneath the concrete bottom (m^2)

ε = porosity (m^3/m^3)

K_d = sorption distribution coefficient (m^3/kg)

ρ_s = solid density of sand/gravel(kg/m^3).

The penetration depth is 2 cm or less for sorbing radionuclides and 125 cm for the two non-sorbing radionuclides ^{129}I and organic ^{14}C.

Release calculations after the phase with expelled gas

A schematic illustration of the release paths after the phase with expelled gas is shown in Figure 6-5. The contamination is in the beginning of this phase distributed inside the waste packages and in part of the sand/gravel in the bottom, corresponding to the penetration depth calculated for the “plug flow phase”. The release mechanisms are as indicated in the figure, diffusion through the porous concrete and concrete structure and both diffusion and water flow in the sand/gravel. The size and direction of the water

flow is the same as in the case with no effects of gas, see previous sub-section and so are material data, geometry and boundary conditions.

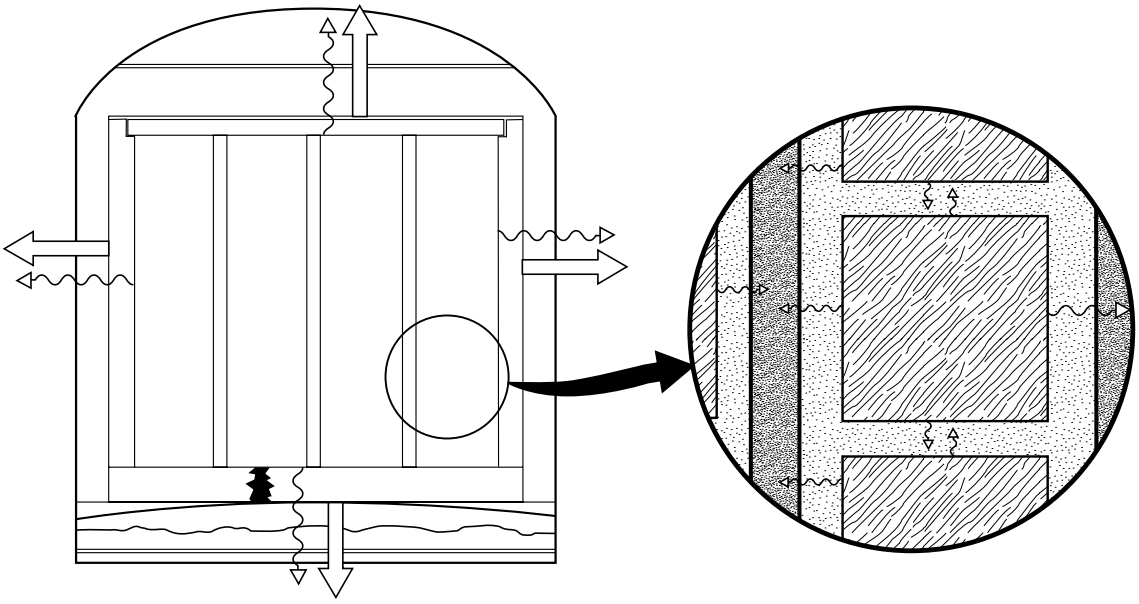

Figure 6-5 Schematic illustration of the release paths in the scenario with expulsion of water through a fracture in the bottom of the concrete structure and out into the sand/gravel backfill.

6.2.3 Case C: Bentonite barriers and displacement of water by gas

In this calculation case it is assumed that the concrete structure and its interior do not constitute any resistance to gas escape, but that an internal overpressure of 50 kPa has to be reached before gas can escape out through the sand/bentonite above the lid of the concrete structure. During this period, water is pushed into the concrete walls and out through the fracture in the bottom. In the calculations this is considered as transport of radionuclides by plug flow. When no more water is displaced, the release of radionuclides takes place by diffusion through the concrete structure and its interior and by diffusion through the bentonite barriers.

Plug flow phase

The total volume of free water in the waste packages in SFL 3 is estimated to be 474 m^3 (see Appendix E). An overpressure of 50 kPa corresponds to a 5 m decrease in the water level inside the concrete structures. The volume of free water that will be displaced is then 5/12 of 474 m^3, i.e. 198 m^3. This water volume is pushed into the walls, the lid and the bottom of the concrete structure as well as through the fracture in the bottom of the structure and out into the sand/bentonite below. The amount of water that flows into the different barriers is determined by calculating the flow resistance in the barriers. To calculate these resistances it is assumed that the fracture is so large that the resistance in the fracture is negligible and that water flowing through the fracture will flow through 10% of the bottom area of the sand/bentonite beneath the concrete bottom. The barrier dimensions used in the calculations are given in Lindgren and Pers, (1994) and in

Appendix G. The hydraulic conductivity in concrete is set to 10^{-9} m/s and in bentonite and sand/bentonite 10^{-10} m/s and 10^{-9} m/s, respectively (Moreno and Neretnieks, 1991). The resistance to flow in the porous concrete surrounding the waste packages is neglected.

Distributing the volume of water expelled between the different barriers according to their relative resistance to flow gives the following results:

Concrete lid: 90 m^3 Concrete walls: 29 m^3

Concrete bottom: 65 m^3 Fracture in concrete bottom: 13 m^3

To calculate the radionuclide transport from the waste packages with plug flow of these volumes of water the potential sorption capacity in the porous concrete is neglected.

The penetration depth into the concrete walls, lid and bottom and into the sand/bentonite beneath the fracture in the concrete bottom is calculated using equation 6-1. This gives the following penetration depths:

Concrete lid: 2 cm or less for sorbing radionuclides and 65 cm for the non-sorbing organic ^{14}C

Concrete walls: 0.3 cm or less for sorbing radionuclides and 10 cm for the non-sorbing organic ^{14}C

Concrete bottom: 1.5 cm or less for sorbing radionuclides and 47 cm for the non-sorbing organic ^{14}C

Sand/bentonite: 13 cm or less for sorbing radionuclides and 42 cm for the non-sorbing organic ^{14}C

Release calculations after the phase with expelled gas

A schematic illustration of the release paths after the phase with expelled gas is shown in Figure 6-6. At the beginning of this phase, the concentration front of the different radionuclides is given by the penetration depths calculated for the plug flow case. The subsequent release of radionuclides occurs by diffusion in the concrete structures and surrounding bentonite barriers. Material data, geometry and boundary conditions used in the calculations are the same as those used for the reference case in the prestudy of SFL 3-5 (Lindgren and Pers, 1994, and Appendix G in this report).

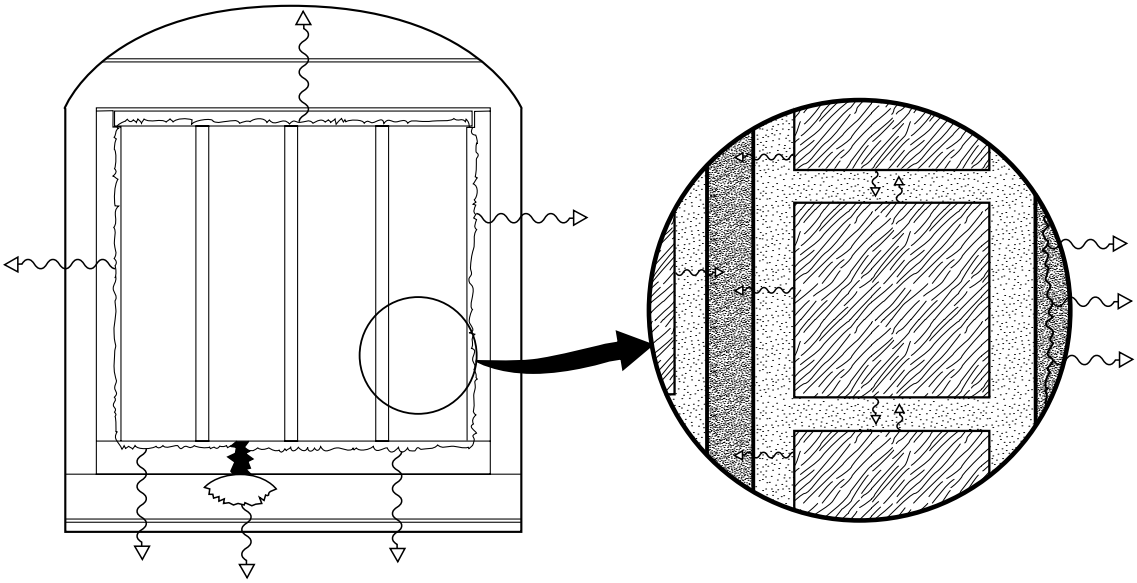

Figure 6-6 Schematic illustration of the release paths in the case with bentonite barriers and expulsion of water by gas.

6.3 Results

The calculated release rates of the radionuclides ^{135}Cs, ^{59}Ni, ^{129}I and organic ^{14}C from the near field are shown in Figure 6-7 for an SFL 3 with a sand/gravel backfill outside the concrete structure. Two curves are displayed for each radionuclide. One shows the release rate in the case where gas can escape without affecting the release (base case) and the other shows the release rate in the case where gas is affecting the release (gas case). The figure shows that displacement of water by gas will result in higher release rates at shorter times, but the maximum release rates of these nuclides from the near field are not affected. The largest difference in release rate at early times is obtained for the non-sorbing radionuclides ^{129}I and organic ^{14}C, while the effect on the release of the slightly sorbing nuclide ^{135}Cs is negligible.

The release rates from the near field of an SFL 3 with bentonite barriers are exemplified in Figure 6-8. Here the release rates obtained for the case with displacement of water are compared with the release rates for the reference case with no effects of gas that is reported in the prestudy of SFL 3-5 (Wiborgh (ed.), 1995 and Lindgren and Pers, 1994). The release of organic ^{14}C in case of bentonite barriers was not calculated within the prestudy of SFL 3-5. Therefore, the release of ^{14}C in case of bentonite barriers is calculated as a part of this study assuming than 10% of the total inventory of ^{14}C is organic and that no sorption takes place in any of the barriers. Figure 6-8 shows that displacement of water by gas will result in a higher release rate of non-sorbing organic ^{14}C at shorter times, but that the maximum release rate is almost the same as in the reference case without water displacement. Similar results are obtained also for the slightly sorbing radionuclides ^{135}Cs and ^{59}Ni.

The maximum release rate from SFL 3 with a sand/gravel backfill is compared to the maximum release rate with bentonite barriers in Table 6-1. Sand/gravel backfill instead of bentonite barriers gives higher maximum release rates of ^{129}I, ^{59}Ni, and organic ^{14}C,

but the difference is smaller than a factor of 10. The opposite result is obtained for ^{135}Cs with a lower maximum release rate in case of a sand/gravel backfill. This is explained by the higher K_d-value used for cesium in sand/gravel than in bentonite and sand/bentonite.

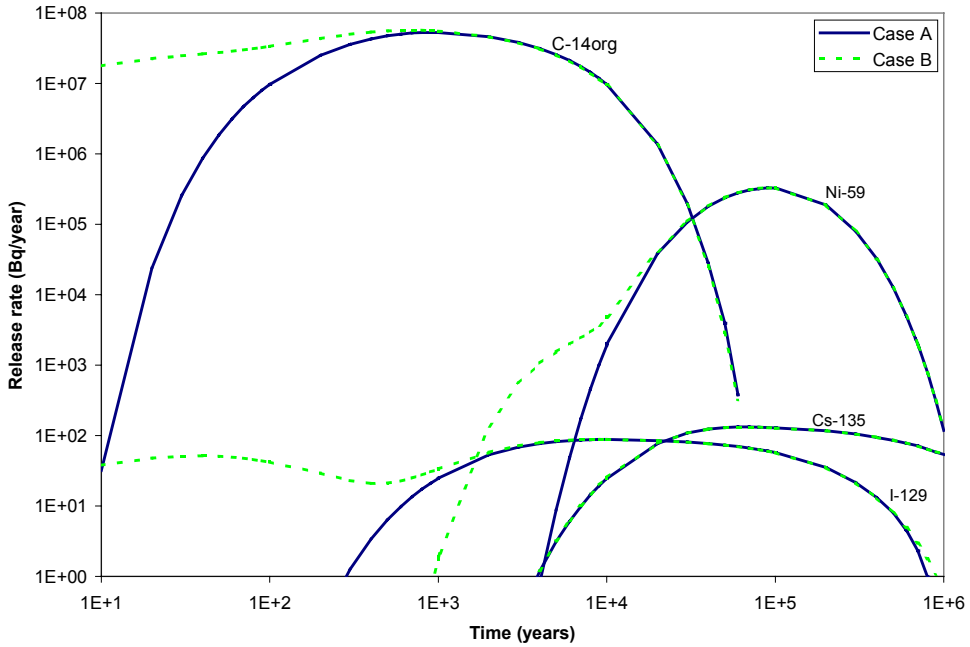

Figure 6-7 Release rates from the near field of SFL 3 when the concrete structure is surrounded by sand/gravel for the case with no displacement of water (Case A) and the case with displacement of water (Case B).

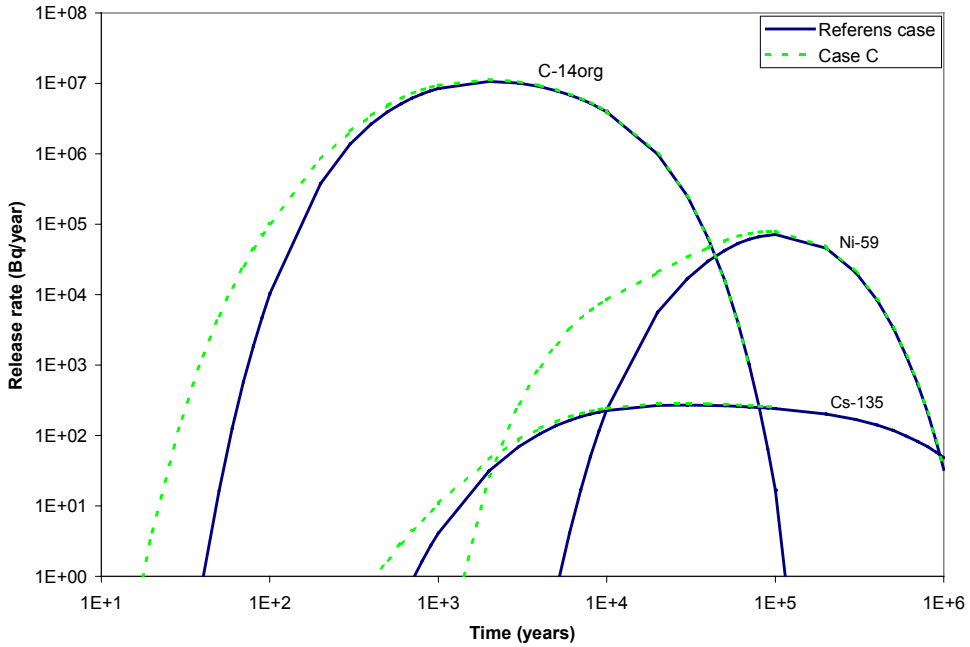

Figure 6-8 Release rates from the near field of SFL 3 when the concrete structure is surrounded by bentonite barriers for the case with no displacement of water (reference case) and the case with displacement of water (case C).

Table 6-1 Maximum release rate from SFL 3 with sand/gravel as outer barrier normalised to the maximum release rate with bentonite barriers. No displacement of water by gas

Nuclide	Half-life	Normalised maximum release rate
C-14org	$5.7 \cdot 10^3$	5
Ni-59	$7.5 \cdot 10^4$	5
I-129	$1.6 \cdot 10^7$	9
Cs-135	$2.3 \cdot 10^6$	0.4

6.4 Concluding remarks

The simple calculations carried out here indicates that a sand/gravel backfill in SFL 3 may lead to higher maximum release rates than obtained with bentonite and sand/bentonite barriers in SFL 3. However, the difference should not be larger than a factor of about 10 as shown by the release rates of the non-sorbing nuclide ^{129}I.

Displacement of water by gas will not affect the maximum release rates of non-sorbing or slightly sorbing radionuclides with moderate or long half-lives, independent of whether sand/gravel or bentonite and sand/bentonite is used as a barrier in SFL 3. This may not be the case for more short-lived radionuclides where the retention time in the near-field barriers is more important for the extent of radioactive decay. Displacement of water by gas will reduce the retention time in the barriers and thus increase the release rates of short-lived radionuclides. However, the release of short-lived radionuclides will most likely be of negligible importance in comparison to the release of long-lived radionuclides even if displacement of water takes place. This is exemplified by comparing the maximum release rates of the short-lived ^{63}Ni with the maximum release rate of the more long-lived ^{59}Ni calculated for the reference case in the prestudy (see Table 7 in Appendix G). This comparison shows that displacement of water must increase the maximum release rate of the short-lived ^{63}Ni with more than 10 orders of magnitude to obtain a maximum release rate of ^{63}Ni that is of the same magnitude as the maximum release rate of ^{59}Ni.

7 Influence of modifications in design and waste inventory on gas generation and pressure build-up

7.1 General

Before the conclusion of this study a modified design concept for the SFL 3-5 repository was proposed and an update of the earlier waste characterisation was initiated. In addition, it was decided to carry out a preliminary safety analysis of the repository concept based on the new proposed design, the updated waste inventory and utilising site-specific data derived for the safety assessment of the deep repository for spent fuel, SR 97. It was therefore decided to make a rough estimate of the impact of these changes in design and waste inventory on the gas generation and pressure build-up estimated for the old design and with the waste inventory derived for the prestudy of SFL 3-5 (Wiborgh (ed.), 1995). The premises for and results of this rough estimate are described in this chapter.

The preliminary safety assessment of SFL 3-5 is carried out for a repository located in Aberg, Beberg and Ceberg at a depth of 300 to 375 m (Munier *et al.*, 1997), while a depth of 500 m was assumed in the prestudy. This change in depth of the location of the repository is not considered here. However, a shallower location of the repository will result in larger gas volumes since the gas volume decreases proportionally with depth. A larger gas volume will also result in higher gas pressure.

7.2 Modifications in design and waste inventory

The new design is described in detail in Forsgren *et al.* (1996) and the updated reference waste inventory in Lindgren *et al.* (1998). Here only the main differences in design and waste inventory are listed, focussing on those entities that affect gas generation, gas pressure build-up and gas escape from the repository.

Regarding the design, the main differences concern SFL 3 and SFL 5. In SFL 3, the bentonite barriers surrounding the concrete encapsulation are replaced by gravel backfill. In addition, there are minor changes in the dimensions of the vault as well as of the concrete structures. In the old design, SFL 5 consisted of three parallel tunnels. In the new design these tunnels are replaced by one vault, identical in dimensions and design to the new SFL 3 vault. The implications of the design modifications on gas generation, pressure build-up and gas escape are:

- The amount of concrete structures in SFL 3 and SFL 5 is smaller and then also the amount of reinforcements that can generate gas via corrosion.
- The space between the waste packages in SFL 5 is backfilled with porous concrete. This will reduce the void accessible to gas inside the concrete structures in SFL 5 compared to the earlier design where no backfill around the waste packages was assumed.

- Gravel backfill surrounding the concrete enclosure in SFL 3 instead of bentonite barriers will decrease the pressure difference required for gas transport from the concrete enclosure to the near-field rock.

The new waste characterisation has resulted in some changes in the estimated amounts of gas generating materials and revised figures on voids in waste packages. In summary the new waste characterisation show:

- Very similar quantity of steel in waste packages in SFL 3, but a 60% larger quantity of aluminium than in the earlier waste inventory. The quantity of organic materials that can generate gas is almost the same, but the distribution between cellulose and other organic materials is different. The quantity of cellulose has decreased to about 50% of the earlier estimate and the quantity of other organic materials is about 7% higher than the earlier estimate.
- A somewhat smaller quantity of steel in waste and waste packages in SFL 4 compared to the earlier estimate.
- A somewhat larger quantity of steel in waste packages in SFL 5 compared to the earlier estimate.
- A somewhat larger internal void (excluding the porosity in cement and concrete) in the waste packages in SFL 3 and SFL 5 compared to the earlier estimate.

The new design data (Forsgren *et al.*, 1996) and the updated reference inventory (Lindgren *et al.*, 1998) are used to make new estimates of gas generation and pressure build-up. Other assumptions are in general the same as those used in the calculations for the old design and waste inventory (see previous chapters). In some cases somewhat different assumptions are made when estimating the total void in the waste packages. These differences are further described in the following sections where also the results of the new estimates are given.

7.3 SFL 3

The main changes in waste inventory and design that affects gas generation in SFL 3 are that the amount of aluminium in the waste is 60 % more than in the earlier estimate and that the amount of concrete structures and thereby also reinforcements is smaller in the new design. The void and free water volumes, that affect the pressure build-up, have also been revised. The earlier estimate of the void and free water volume inside the inner packaging was calculated by assuming a total porosity of 0.4 to 0.5 for the different waste types. The free water volume inside the inner packaging was assumed to be 30 % of the porosity in conditioned waste and 100 % of the porosity in unconditioned waste (see 5.1.2). In the updated waste inventory the empty space in the waste packages is specified. This information together with the assumption that the porosity of the waste is 20 % is used to estimate the total void in the waste packages. The free water volume inside the inner packaging is assumed to be the empty space and 30 % of the porosity in conditioned waste and 100 % of the porosity in unconditioned waste. These assumptions result in a total void in the packages that is 4% larger than earlier and a free water volume that is 80 % larger than earlier.

The initial gas generation rate is calculated to be 446 m^3/year, i.e. 20% higher than for the old design and earlier waste inventory. This is mainly due to the larger amount of aluminium in the new waste inventory.

The total volume of gas produced in SFL 3 is calculated to be 90% of the volume estimated for the old design and earlier waste inventory. This is mainly due to a smaller amount of concrete structures in the new design. The gas formed by corrosion of reinforcements in the concrete structures is 56 % of the volume generated in the old design. However, the volume of gas produced in waste and packaging is somewhat larger than earlier. The volume of gas produced as a function of time is shown in Figure 7-1. The corresponding results for the old design and earlier waste inventory are given in Figure 5-4 and Table 5-2.

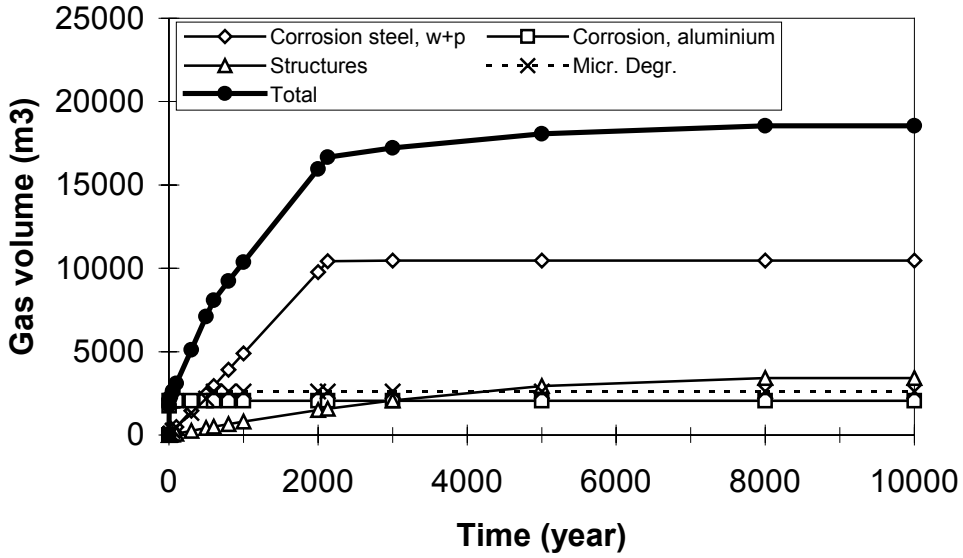

Figure 7-1 Gas volumes at repository depth (500 m) generated by corrosion of aluminium in waste, steel in waste packages (w+p) and reinforcement in concrete structures and by microbial degradation of organic materials in the waste in SFL 3 .

The pressure build-up inside the waste packages can be divided into two parts a fast build-up during the first 5 years governed by corrosion of aluminium and thereafter a slower build-up. The pressure build-up inside the waste packages during the first five years is higher than in the earlier estimate if the total void is accounted. This is because of the larger amount of gas-generating aluminium in the waste and approximately the same void in the waste packages. If only the free water volume is considered to be accessible to gas, approximately the same pressure build-up is achieved as in the earlier estimate. The reason for this is that the larger volume of free water compensates the larger volume of gas generated during the first five years.

At longer times when the aluminium has corroded away, the over pressure inside the waste packages is almost the same as in the earlier calculations if the total void in the waste packages is considered as being accessible to gas. If only the volume of free water

in the packages is available to gas, the over pressure at longer times is lower, 56 % of the pressure reached in the earlier calculations. The explanation to this is that the accumulated gas volume becomes more and more similar once the aluminium has corroded away, in combination with a larger volume of free water in the new calculations. The pressure build-up in the waste packages as a function of time is shown in Figure 7-2. The corresponding results for the earlier waste inventory is shown in Figure 5-6.

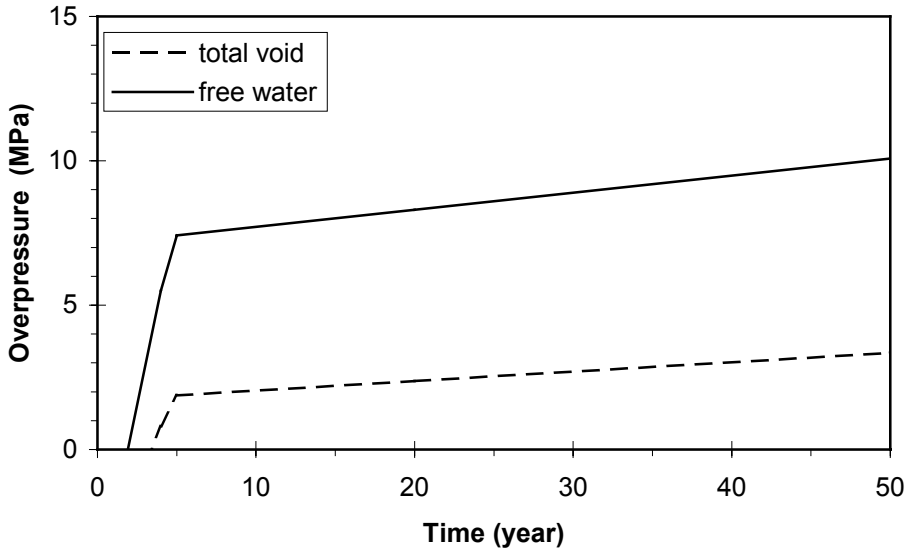

Figure 7-2 Overpressure at repository depth (500 m) in packages in SFL 3.

The pressure build-up in the concrete building as a function of time is shown in Figure 7-3 (corresponding to Figure 5-5 in the earlier calculations). The pressure build-up is slower than in the earlier calculations if only the free water volume is considered as accessible to gas. The final pressure is also lower, only 40 % of the pressure reached in the calculations for the old design and earlier waste inventory. This is mainly because the volume of free water is larger than in the earlier calculations. If the total void is accessible to gas, the pressure build-up at longer times is similar to the pressure build-up estimated for the old design and earlier waste inventory. This is to be expected since the difference in both the total gas volume and total void is small.

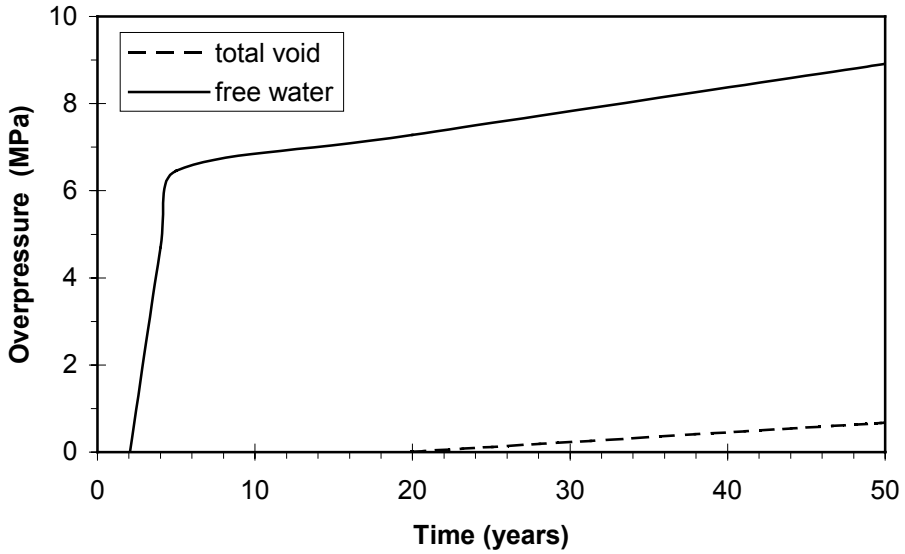

Figure 7-3 Overpressure at repository depth (500 m) in the concrete building in SFL 3.

In summary the calculations show that the new design and updated waste inventory may lead to somewhat different gas volumes and pressure build-up in SFL 3 compared to the old design and earlier waste inventory. However, the new results still indicate that the internal gas pressure within a short time period will open up cracks or slits in the waste packages and concrete structures if these initially are intact. Regarding the gas escape from SFL 3, the major difference is most likely related to the replacement of the bentonite barriers with a gravel backfill. A few small cracks or slits in the concrete structure will allow gas to escape through the structure and gravel backfill already at a small pressure difference. A larger pressure difference, of the order of 50 kPa, is required for gas to escape if a sand/bentonite barrier is placed above the lid of the concrete structure.

7.4 SFL 4

The updated waste inventory for SFL 4 is very similar to the earlier waste inventory. The total volume of gas generated is calculated to be somewhat smaller using data from the updated inventory. The calculations carried out for the earlier inventory should then be representative also for the updated inventory.

7.5 SFL 5

The main changes in waste inventory and design that affects gas generation in SFL 5 are that the estimated amount of steel in the waste packages is larger in the updated inventory and that the design is changed from three smaller vaults to one bigger vault. The amount of reinforced concrete structures is somewhat smaller in the new design and thereby also the amount of reinforcements that generates gas. The total void and volume of free water is also different. In the updated waste inventory the empty space in the waste packages is reported to be 40% larger than the value estimated from the earlier

waste inventory. In the new design, the waste packages are surrounded by porous concrete. This was not the case in the old design. This means that both the total void and volume of free water are smaller in the new design (waste packages excluded) compared to the old design (waste packages excluded).

The initial gas generation rate is calculated to be some few percent higher for the new design and updated waste inventory and the estimated total volume of gas that can be generated is approximately 2 % larger. This is mainly due to the larger amount of steel in the waste packages in the updated inventory. The new design of the concrete structure comprises less material and hence the gas produced by the concrete structure is less than in the earlier calculations. The gas produced as a function of time is shown in Figure 7-4. The corresponding results for the old design and earlier waste inventory are shown in Figure 5-12.

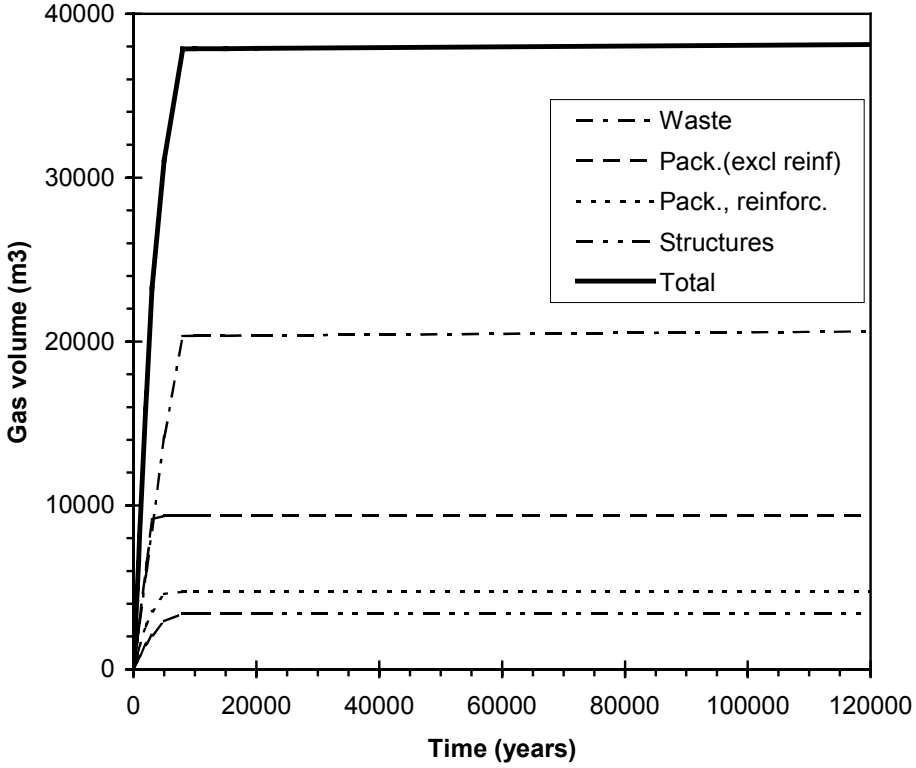

Figure 7-4 Volumes of hydrogen gas generated at repository depth (500 m) by corrosion of steel and Zircalloy in SFL 5.

The pressure build-up in the waste packages is about 15 % lower than in the earlier calculations if the total void is assumed to be accessible to gas. The difference is even larger 18 % if only the volume of free water is available to gas. This is mainly due to the new estimate of the empty space inside the cassettes in the waste packages. The pressure build-up in the waste packages as a function of time is shown in Figure 7-5. The corresponding results for the earlier waste inventory are shown in Figure 5-13.

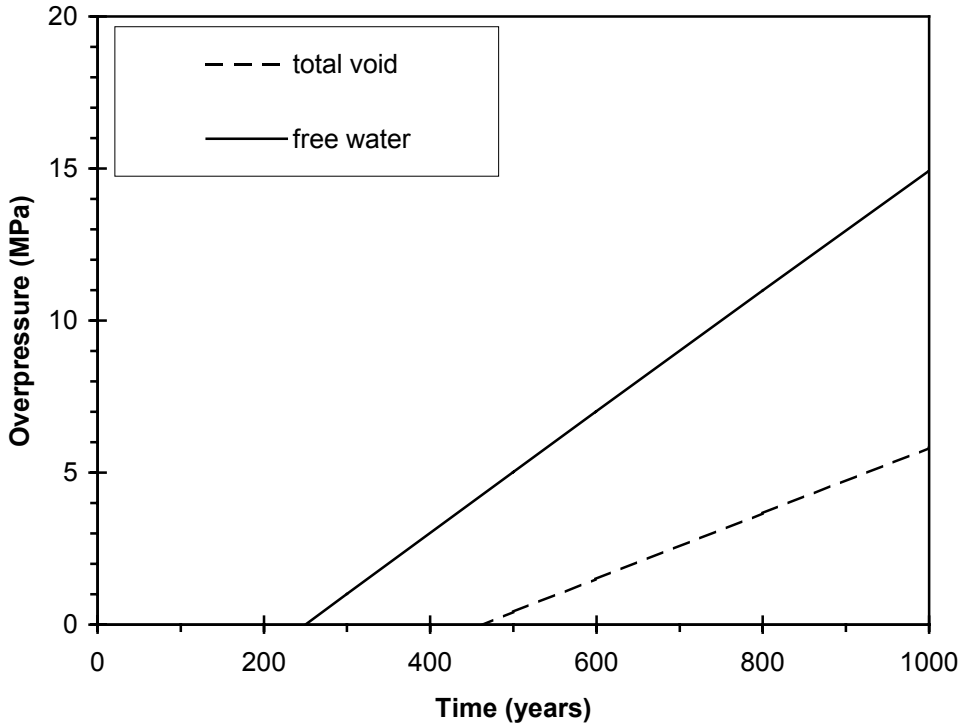

Figure 7-5 Overpressure at repository depth (500 m) in the waste packages in SFL 5.

The pressure build-up inside the concrete structure is much faster and reaches a higher value in the new design compared to the old design. The maximum pressure is almost 2 times higher if the total void is accessible to gas and more than 2 times higher if the volume of free water is accessible to gas. The new design with porous concrete between the waste packages will reduce the volume accessible to gas and hence give higher internal gas pressure. The pressure build-up inside the concrete structures for the new design and updated waste inventory is shown in Figure 7-6 and the corresponding results for the old design and earlier waste inventory in Figure 5-14.

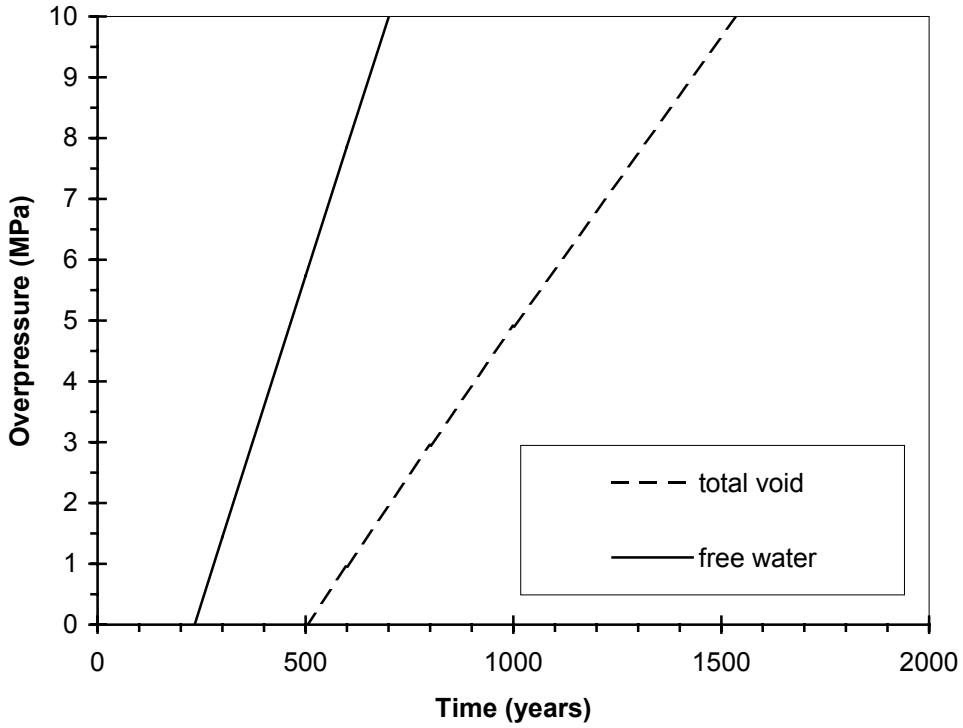

Figure 7-6 Overpressure at repository depth (500 m) in the concrete building in SFL 5.

In summary, the calculations show that the gas generation is similar for the new design and updated waste inventory, but that the pressure build-up is faster than for the old design and earlier waste inventory. The implication of the difference in pressure build-up is that cracking of the concrete structures in SFL 5 could take place at an earlier time than estimated for the old design and earlier waste inventory. However, this is only the case if the concrete initially is intact and gas tight.

8 Conclusions

Calculations of gas generation inside the waste packages in SFL 3 for the same repository design and waste inventory as in the prestudy of SFL 3-5 show a quick pressure build-up inside the waste packages if they initially are gas tight. Based on the calculated gas pressure build-up it seems reasonable to assume that even if the waste packages initially are gas tight, the internal gas pressure will cause cracks through which the gas may escape. This may occur within the first few tens of years after repository closure. The same conclusions can be drawn for the concrete structure even though the time for the pressure build-up is longer. Cracking of the structures is to be expected within the first 200 years of gas generation.

Provided that the gas transport capacity in the surrounding rock not is a limiting factor the performed calculations show that the sand-bentonite will determine the gas escape. Once the gas pressure has reached the capillary pressured required for displacement of water in the pores in the sand/bentonite layer, only a small part of the porosity is needed for gas to escape through the sand/bentonite at the same rate as it is generated.

Simple calculations suggest that gas escape from the waste contained in SFL 4 probably will occur without major internal pressure build-up. The maximum internal overpressure will most likely be determined by the pressure required to displace water in the largest pores in the sand/gravel backfill thereby open up gas channels in the backfill. This capillary pressure is dependent on the particle size distribution of the backfill. Data in the literature on capillary pressures in similar materials indicate that the internal overpressure probably not will be higher than 0.1 to 1 kPa, as long as more clay type materials are avoided.

For SFL 5 it seems reasonable to assume that even if the waste packages and concrete structures are intact initially, the internal pressure build-up will create cracks or fractures at a lower internal overpressure than 1 MPa. With a waste inventory and design as in the prestudy of SFL 3-5 (Wiborgh (ed.), 1995) this overpressure is calculated to be reached within 500 years of gas generation for the waste packages and within 1 000 years of gas generation for the concrete structure.

The concrete structures in the SFL 5 vaults are surrounded by sand/gravel backfill of similar type as in SFL 4. The initial gas generation rate in SFL 5 is about 3 times lower than in SFL 4 and the geometry of the backfill on top of the waste are similar. Thus, the simple calculations made of the gas transport capacity in the sand/gravel backfill in SFL 4 are valid also for SFL 5. This means that the pressure difference required for creating gas channels in the backfill in SFL 5 probably not will be higher than 0.1 to 1 kPa.

Some simple calculations of the radionuclide release from SFL 3 indicate that gas pressure build-up and displacement of water not will affect the maximum release rates of important radionuclides from the near field. This is the case irrespective of sand/bentonite and bentonite or sand/gravel outside the concrete structure in an SFL 3 vault with the same waste inventory and dimensions as in the prestudy of SFL 3-5 (Wiborgh (ed.), 1995). However, replacing the bentonite barriers with sand/gravel may result in higher maximum release rates of non-sorbing radionuclides with at most a factor of about 10. The effect on the release of other radionuclides depends on the

relation between their sorption capability in the different barrier materials and on their half-lives.

Before the conclusion of this study a modified design concept for the SFL 3-5 repository was proposed and the earlier waste characterisation was updated. Rough estimates of the impact of these changes in design and waste inventory show some differences in generated gas volumes and pressure build-up in SFL 3 and SFL 5 if gas cannot escape from the waste packages and concrete structures. The results for SFL 4 are very similar. Despite the differences in results for SFL 3 and SFL 5, the conclusion drawn based on the more detailed calculations for the old design and earlier waste inventory is still valid. If gas accumulated inside the concrete structures the build-up of gas pressure will within a short time period open up slits or crack the concrete to allow gas to escape. The major difference between the old and new design is related to the replacement of the bentonite barriers with a gravel backfill. Even if gas can escape through the concrete structure in SFL 3 without a major increase in pressure, bentonite barriers surrounding the structure will always imply an internal pressure build-up that is higher than the pressure build-up in case of sand/gravel outside the structures. The reason for this is that the capillary pressure in a sand/bentonite barrier is larger than in a sand/gravel backfill.

The preliminary safety assessment of SFL 3-5 is carried out for a repository located in Aberg, Beberg and Ceberg at a depth of 300 to 375 m. All results given in this report are for a repository depth of 500 m. A shallower location of the repository will result in larger gas volumes and faster pressure build-up, but this will not change the above conclusions.

References

Brandberg S, Wiborgh M, 1982. Långtidsförändringar i SFR, SFR Progress Report SFR 81-10, Swedish Nuclear Fuel and Waste Management Co, Stockholm. (in Swedish)

Collin M, Rasmuson A, 1986. Distribution and flow of water in unsaturated layered cover materials for waste rock. National Swedish Environmental Protection Board Report 3088, Stockholm.

Forsgren E, Lange F, Larsson H, 1996. SFL3-5, Layoutstudie. SKB Arbetsrapport AR D-96-016, Swedish Nuclear Fuel and Waste Management Co, Stockholm.

Höglund L O, Bengtsson A, 1991. Some chemical and physical processes related to the long-term performance of the SFR repository. SFR Progress Report SFR 91-06, Swedish Nuclear Fuel and Waste Management Co, Stockholm.

Höst-Madsen, 1989. Immiscible multi- phase flow in porous media. Institute of Hydrodynamics and Hydraulic Engineering, Technical University of Denmark, Series paper no.49, Lyngby, Denmark.

Munier R, Sandstedt H, Niland L, 1997. Förslag till principiella utformningar av förvar enligt KBS-3 för Aberg, Beberg och Ceberg. SKB rapport R-97-09, Swedish Nuclear Fuel and Waste Management Co, Stockholm. (in Swedish)

Lindgren M, Brodén K, Carlsson J, Johansson M, Pers K, 1994. Low and intermediate level waste for SFL 3-5. SKB Arbetsrapport AR 94-32, Swedish Nuclear Fuel and Waste Management Co, Stockholm.

Lindgren M, Pers K, 1994. Radionuclide release from the near-field of SFL 3-5, A preliminary study. SKB Arbetsrapport AR 94-54, Swedish Nuclear Fuel and Waste Management Co, Stockholm.

Lindgren M, Pers K, Skagius K, Wiborgh M, Brodén K, Carlsson J, Riggare P, Skogsberg M, 1998. Low and intermediate level waste in SFL 3-5: Reference inventory. SKB Reg. No:19.41/DL31, Swedish Nuclear Fuel and Waste Management Co, Stockholm.

Moreno L, Neretnieks I, 1991. Some calculations of radionuclide release from the silo repository. SFR Progress Report SFR 91-07, Swedish Nuclear Fuel and Waste Management Co, Stockholm.

PLAN93, 1993. Plan93 Costs for management of the radioactive waste from nuclear power production. SKB TR 93-28, Swedish Nuclear Fuel and Waste Management Co, Stockholm.

Wiborgh M, Höglund L O, Pers K, 1986. Gas formation in a L/ILW repository and gas transport in the host rock. Nagra Technical Report NTB 85-17, Wettingen, Switzerland.

Wiborgh M (ed.), 1995. Prestudy of final disposal of long-lived low and intermediate level waste. SKB Technical Report TR 95-03, Swedish Nuclear Fuel and Waste Management Co, Stockholm.